Journal of Nonlinear Science (2024) 34:84
https://doi.org/10.1007/s00332-024-10062-2

Journal of Nonlinear Science

Mathematical Models for the Large Spread of a Contact-Based Infection: A Statistical Mechanics Approach

Marzia Bisi[1] · **Silvia Lorenzani**[2]

Received: 5 January 2024 / Accepted: 25 June 2024 / Published online: 8 July 2024

Abstract
In this work, we derive a system of Boltzmann-type equations to describe the spread of contact-based infections, such as SARS-CoV-2 virus, at the microscopic scale, that is, by modeling the human-to-human mechanisms of transmission. To this end, we consider two populations, characterized by specific distribution functions, made up of individuals without symptoms (population 1) and infected people with symptoms (population 2). The Boltzmann operators model the interactions between individuals within the same population and among different populations with a probability of transition from one to the other due to contagion or, vice versa, to recovery. In addition, the influence of innate and adaptive immune systems is taken into account. Then, starting from the Boltzmann microscopic description we derive a set of evolution equations for the size and mean state of each population considered. Mathematical properties of such macroscopic equations, as equilibria and their stability, are investigated, and some numerical simulations are performed in order to analyze the ability of our model to reproduce the characteristic features of Covid-19 type pandemics.

Keywords Boltzmann equation · Kinetic theory · Epidemiological models · Living systems · Nonlinearity

Mathematics Subject Classification 35Q20 · 82C40 · 92D30

1 Introduction

The history of mathematical models in epidemiology begins with the paper "*Essai d'une nouvelle analyse de la mortalité causée par la petite vérole*" written by Daniel

Communicated by Pierre Degond.

✉ Silvia Lorenzani
silvia.lorenzani@polimi.it

[1] Dipartimento di Scienze Matematiche, Fisiche e Informatiche, Università di Parma, Parco Area delle Scienze 7/A, 43124 Parma, Italy

[2] Dipartimento di Matematica, Politecnico di Milano, Piazza Leonardo da Vinci 32, 20133 Milan, Italy

Bernoulli in 1766 to analyze the mortality due to smallpox in England (Bernoulli 1766). In this paper, Bernoulli derived a model showing that inoculation against the virus would increase the life expectancy. Following the work of Bernoulli, Lambert in 1772 extended the model by incorporating age-dependent parameters (Lambert 1772). However, this kind of approach has not been developed systematically until 1911 when the British medical doctor Ronald Ross published the paper "The prevention of malaria," considered the starting point of the modern mathematical epidemiology (Ross 1911). For the first time, in this work, a set of differential equations were derived to study the discrete-time dynamics of mosquito-borne malaria. Similar epidemic models were later developed by Kermack and McKendrick, who founded the deterministic compartmental modeling (Kermack and McKendrick 1927, 1932, 1933). These authors proposed the celebrated SIR model according to which the population is divided into three groups or compartments: the susceptible (S), who can contract the disease, the infected (I), who have already contracted the disease and can transmit it, and the recovered (R), who are healed. Within this framework, it is assumed that the probability of infection of a susceptible is proportional to the number of its contacts with infected individuals. The resulting mathematical model, based on a deterministic system of ordinary differential equations, relies on the following hypotheses: (i) a homogeneous mixing of the contacts; (ii) the conservation of the total population; (iii) relatively low rates of interaction. Over the years, SIR-type models have been extended to include age-dependent infection, mortality, and spatial dependence of the epidemic spread (Siettos and Russo 2013; Zhang et al. 2023; Zhang and Zheng 2023).

However, since the classical epidemiological models are derived at a macroscopic level, they neglect the heterogeneity of disease transmission due to the microscopic features of the interactions between individuals. Relying on recent developments of kinetic models for the description of social and economic phenomena (Dimarco and Toscani 2019; Pareschi and Toscani 2013; Toscani 2020), in the last few years a number of works have appeared aimed at connecting the distribution of social contacts with the spreading of a disease in a multi-agent system. A historical review on the attempts of modeling social phenomena by means of the laws of statistical physics may be found in Ball (2002); Patriarca and Chakraborti (2013); more specifically, analogies and differences between the classical Boltzmann approach to gas dynamics and kinetic models for socio-economic sciences are discussed in detail in Fraia and Tosin (2021). Many papers are available on the derivation of macroscopic epidemic models accounting also for interrelations between individuals and social features (Bellomo et al. 2020; Bertaglia and Pareschi 2021; Boscheri et al. 2021; Dimarco et al. 2020, 2021). These studies have been usually carried out by integrating a classical compartmental model (typically a SIR-type model) with a statistical part based on Boltzmann-like equations describing the formation of social contacts. Such an approach allows one to obtain various sub-classes of macroscopic epidemiological models characterized by nonlinear incidence rates. Within the same mathematical framework of multi-agent systems, a different procedure has been considered in Della Marca et al. (2022, 2023); Kim and Quaini (2020), where kinetic evolution equations have been derived for the distribution functions of the viral load of the individuals that change as a consequence of binary interactions or interactions with a background. But also in Della Marca et al. (2022,

2023) a SIR-like compartmental structure has been obtained in order to describe the evolution of the pandemic.

In the present paper, following the general setting put forward in Delitala (2004); De Lillo et al. (2009), we derive a system of Boltzmann-type evolution equations for the distribution function $f_i(t, u_i)$ $(i = 1, 2)$ of two interacting populations, where the index $i = 1$ refers to individuals without symptoms and $i = 2$ to infected people with symptoms. Unlike the kinetic models mentioned above, in our work the microscopic variable $u_i \in (-\infty, +\infty)$ indicates the level of the infection, so that the product $f_i(t, u_i)\, du_i$ gives the number of individuals of the i-th population which at the time t are in the elementary state $[u_i, u_i + du_i]$. Within the population described by the distribution function $f_1(t, u_1)$, we can distinguish healthy individuals, when $u_1 < 0$, and positive asymptomatic, when $u_1 \geq 0$. Similarly, the population represented by the distribution function $f_2(t, u_2)$ is made up of positive symptomatic, when $u_2 < 0$, and hospitalized individuals, when $u_2 \geq 0$. Our approach does not rely on one of the existing classical compartmental models (Buonomo and Giacobbe 2023; Della Marca et al. 2022, 2023; D'Onofrio and Manfredi 2022), where infected people have been assigned to a unique compartment, but we tried to emphasize the crucial role played by positive asymptomatic individuals in the spread of a contact-based infection, as recently observed in the evolution of Covid-19.

The idea behind our derivation is to treat interactions between individuals in the same way as those between molecules of chemically reacting gas mixtures. In particular, the transition from population 1 (made up of individuals without symptoms) to population 2 (made up of infected individuals with symptoms) is described by using the same formalism used in classical kinetic theory of gases when two interacting particles change their nature. The reverse transition in our model is taken into account when the medical staff (belonging to population 1) interacts with positive symptomatic or with people hospitalized (belonging to population 2) giving rise to their recovery. We also consider the action of the immune system modeled in close analogy to the interaction of a particle (a single person) with a background (the immune system), typical of the neutron transport description in kinetic theory (Cercignani 1988). The major mathematical difficulty in our model consists in deriving a system of four macroscopic equations for the evolution of the number densities and mean states of healthy people, positive asymptomatic, positive symptomatic, and hospitalized persons, starting from a set of two Boltzmann equations defined at the microscopic level for the distribution functions f_1 and f_2. The closure of such macroscopic system is based on specific choices of Boltzmann collision kernels and of interaction rules that, as usual in multi-agent systems involving human beings, also show stochastic effects.

The rest of the paper is organized as follows. In Sect. 2, we present the epidemiological model derived at the microscopic level by setting a system of Boltzmann-like equations. In Sects. 3 and 4, we obtain the macroscopic equations for the evolution of the size and mean state, respectively, of each population considered, that is, healthy individuals, positive asymptomatic, positive symptomatic, and hospitalized individuals. These macroscopic equations are then qualitatively analyzed. In particular, the equilibrium states and their stability are investigated in Sects. 5 and 6, respectively. Section 7 presents numerical test cases carried out in order to analyze the ability of our model to reproduce the characteristic features of Covid-19 type pandemics. Some

concluding remarks, mainly aimed at highlighting the novelty of our approach, are included in Sect. 8. Finally, in Appendix we introduce some preliminaries on the scattering kernel formulation of the Boltzmann equation used in this paper.

2 Mathematical Formulation

We derive a model describing the spread of contact-based infections such as SARS-CoV-2 virus within the general mathematical framework of the kinetic theory for multi-species problems (Rossani and Spiga 1999). The system consists of two populations of interacting individuals. Each population is denoted by the subscript i ($i = 1, 2$), according to the following classification:

$$\begin{cases} i = 1 : \text{individuals without symptoms} \\ i = 2 : \text{infected individuals with symptoms.} \end{cases} \tag{1}$$

Within the same population, each individual is characterized by a microscopic state, which is a scalar variable $u_i \in (-\infty, +\infty)$ (activity) (Delitala 2004; De Lillo et al. 2009). Let us introduce the one-particle distribution function: $f_i = f_i(t, u_i)$. By definition, the product

$$f_i(t, u_i)\, du_i$$

gives the number of individuals of the i-th population which at the time t are in the elementary state $[u_i, u_i + du_i]$. The variable u_i depends on the intensity level of a certain pathological state. We distinguish the following cases:

$$f_1(t, u_1) : \begin{cases} \text{if } u_1 < 0 \rightarrow \text{healthy individuals} \\ \text{if } u_1 \geq 0 \rightarrow \text{positive asymptomatic} \end{cases} \tag{2}$$

$$f_2(t, u_2) : \begin{cases} \text{if } u_2 < 0 \rightarrow \text{positive symptomatic} \\ \text{if } u_2 \geq 0 \rightarrow \text{hospitalized individuals.} \end{cases} \tag{3}$$

Specifically, within the same population, the larger is the value of u_i, the stronger is the infection.

The evolution of the system is determined by microscopic interactions between pairs of individuals, which modify the probability distribution over the state variable and/or the size of the population. The system is homogeneous in space, and only binary interactions are taken into account. In addition, we model also the action of the immune system described by the distribution function $\phi_i(v)$ $(i = 1, 2)$ over the microscopic variable $v \in [-M, +M]$, where M is a constant such that $M >> 1$. The values assumed by v are related to different levels of response of the immune system. Furthermore, we consider a finite range for v only for technical reasons. Indeed, one has to require the existence of the integrals involving the distribution function $\phi_i(v)$, which can be modeled as done, for instance, in De Lillo et al. (2009).

We distinguish between two natural actions:

(i) The innate immunity.
Viruses that enter the body can be stopped right away by the innate immune system. The effectiveness of this type of action is linked to the possibility that an individual belonging to population 1 becomes ill or not.
(ii) The adaptive immunity.
The adaptive immune system takes over if the innate immune system is not able to destroy invaders such as viruses. It is slower to respond than the innate immune system, but it identifies specific pathogens and it is able to "remember" them. To the adaptive immunity can be ascribed the recovery of an individual belonging to population 2 even in the absence of specific care.

The current knowledge about SARS-CoV-2 infection indicates that the immune system plays a crucial role in setting the severity of Covid-19. Appropriate immune responses against SARS-CoV-2 could mitigate the symptoms of Covid-19 and prevent the occurrence of a severe disease, while excessive responses trigger pathogenic cell activation increasing the risk of death. In a recent study (the first of its kind), carried out by a large group of researchers, the genome of over 780,000 cells of the immune system was sequenced and the membrane proteins as well as the receptors present on their surfaces were analyzed (Stephenson 2021). These samples, taken from 130 patients with varying severities of Covid-19, revealed a high concentration of B lymphocytes (cells that produce antibodies) and helper T cells (which activate other immune components) in the blood of asymptomatic and paucisymptomatic individuals. On the contrary, analyzing the immune response in patients with critical disease, the researchers identified much lower levels of these cells and a higher concentration of other cells responsible for protecting the body from infection, such as monocytes and killer T lymphocytes. Their uncontrolled increase could be the cause of the excessive inflammatory response at the lung level, in severe cases of Covid-19 infection: a cytokine storm that attacks all the patient's organs, leading to death. Higher concentrations of platelets were also found in the blood of the most seriously ill patients, responsible for the formation of thrombi capable of obstructing the blood flow to the tissues. Although it is not yet clear on what basis the infection triggers different immune responses, this study reveals that the types of cells that are preferentially activated differ from person to person in an unpredictable way.

We will consider the following moments of the distribution functions.

(a) The size of the ith population at time t:

$$n_i(t) = \int_{-\infty}^{+\infty} f_i(t, u_i)\, \mathrm{d}u_i, \quad i = 1, 2 \tag{4}$$

where $n_1 = n_1^{HE} + n_1^A$ and $n_2 = n_2^S + n_2^{HS}$, with

$$n_1^{HE} = \int_{-\infty}^{0} f_1(t, u_1)\, \mathrm{d}u_1 : \quad \text{number density of healthy individuals} \tag{5}$$

$$n_1^A = \int_0^{+\infty} f_1(t, u_1)\,\mathrm{d}u_1 : \quad \text{number density of asymptomatic} \tag{6}$$

$$n_2^S = \int_{-\infty}^{0} f_2(t, u_2)\,\mathrm{d}u_2 : \quad \text{number density of symptomatic} \tag{7}$$

$$n_2^{HS} = \int_0^{+\infty} f_2(t, u_2)\,\mathrm{d}u_2 : \quad \text{number density of hospitalized individuals.} \tag{8}$$

The total number of individuals at time t is given by:

$$N = \sum_{i=1}^{2} n_i(t). \tag{9}$$

Since in this work we are mainly interested in modeling the transmission mechanism of the disease, we will neglect changes in the social structure such as the aging process, births, and deaths. This conservation property implies that N is a constant.

Furthermore, the overall action of the immune system on the individuals of the ith population is given by

$$\hat{I}_i = \int_{-M}^{+M} \phi_i(v)\,\mathrm{d}v, \quad i = 1, 2. \tag{10}$$

Higher-order moments provide additional information on the (macroscopic) description of the system.

(b) Progression of the epidemiological state:

$$U_i(t) = \int_{-\infty}^{+\infty} u_i\, f_i(t, u_i)\,\mathrm{d}u_i \quad i = 1, 2, \tag{11}$$

and the mean viral load of population i, defined as

$$\hat{U}_i(t) = \frac{U_i(t)}{n_i(t)} = \frac{1}{n_i} \int_{-\infty}^{+\infty} u_i\, f_i(t, u_i)\,\mathrm{d}u_i \quad i = 1, 2. \tag{12}$$

The evolution equations for the distribution functions $f_i(t, u_i)$ can be obtained following the formalism of multi-species Boltzmann equations outlined in Appendix. In order to derive these equations, we consider the following hypotheses on interaction processes:

(H.1) the medical staff belongs to the population 1, with $u_1 \in [-\infty, 0[$, and never becomes positive asymptomatic or ill when interacting with sick people belonging to population 2;

(H.2) the interactions produce a smooth shift toward higher pathological states (e.g., a healthy person does not immediately become ill but positive asymptomatic);
(H.3) all positive symptomatic individuals are in isolation and, therefore, they can only have interactions with family members (also positive symptomatic) and with the medical staff;
(H.4) hospitalized individuals can only have interactions between themselves and with the medical staff.
Relying on these assumptions, we describe the interactions within the same population or between different populations as follows.

- Interactions within the population 1.
  (a) Healthy individuals + healthy individuals
  $\longrightarrow$ both individuals remain healthy (population 1);
  (b) Healthy individuals + positive asymptomatic:
  besides the interactions in which individuals do not change category, it may occur the transition healthy individual $\longrightarrow$ positive asymptomatic (population 1);
  (c) Positive asymptomatic + positive asymptomatic:
  it could happen that both remain positive asymptomatic, or that one undergoes the transition positive asymptomatic $\longrightarrow$ positive symptomatic (population 2).
- Interactions within the population 2.
  (d) Positive symptomatic + positive symptomatic:
  one of them could be subject to the change positive symptomatic $\longrightarrow$ hospitalized individual (population 2);
  (e) Hospitalized individuals + hospitalized individuals: $\longrightarrow$ both individuals remain hospitalized (population 2).
- Interactions between the populations 1 and 2.
  Only the medical staff interacts with positive symptomatic or with hospitalized people. Besides interactions where the ill individuals do not change their category, we have the following ones giving rise to recovery:
  (f) Healthy individual (medical staff) + positive symptomatic $\longrightarrow$ healthy individuals (transition to population 1);
  (g) Healthy individual (medical staff) + hospitalized individuals $\longrightarrow$ healthy individuals (transition to population 1).

Therefore, we shall deal with a system of two populations $(1, 2)$ which can also interact according to the following reversible transition, giving rise to a switch from one sub-population to the other:

$$1 + 1 \rightleftarrows 2 + 1 \tag{13}$$

In addition to the interactions between individuals, we consider also those between an individual and the immune system, modeled in close analogy to the interaction of a particle with a background, typical of the neutron transport phenomena in kinetic

theory (Cercignani 1988). In particular, we assume that among the individuals in population 1, only asymptomatic carriers 'interact' with their innate immune system with the probability to become positive symptomatic (transition to population 2). Furthermore, we assume that people belonging to population 2 (both positive symptomatic and hospitalized individuals) interact with their adaptive immune system with a probability of recovery (transition to population 1 among healthy individuals). While the interactions between individuals are described by the full nonlinear Boltzmann operator, those between a person and the immune system give rise to a linear collision operator.

2.1 Derivation of Boltzmann-Type Equations

In the following, we consider the scattering kernel formulation of the Boltzmann collision operator (see Appendix) for both classical interactions without transfers (Q_{ik}) and interactions with switches ($\overline{Q}_i^{(r)}$), or with the immune system ($\overline{L}_i^{(r)}$). In particular, the operators Q_{ii} $(i = 1, 2)$ describe the interactions between individuals within the same population i without a transfer to the other population; the operators Q_{12} and Q_{21} model the interactions between the medical staff (belonging to population 1) and sick people (belonging to population 2) which do not produce any change of category, while the operators $\overline{Q}_i^{(r)}$ account for those interactions between individuals which give rise to a transition from one population to the other; finally, the operators $\overline{L}_i^{(r)}$ take into account the interactions of persons belonging to population i with the immune system. The superscript (r) denotes the non-classical Boltzmann operators, taking into account switches (called "reactions" in gas dynamics) or interactions with a "background" (immune system).

Thus, we get for population 1:

$$\frac{\partial f_1}{\partial t}(t, u_1) = Q_{11} + Q_{12} + \overline{Q}_1^{(r)} + \overline{L}_1^{(r)} \tag{14}$$

where

$$\begin{aligned} Q_{11} \;=\; & \int_{-\infty}^{+\infty}\int_{-\infty}^{+\infty} \eta_{11}(u_*, u^*)\, A_{11}^{(1)}(u_*, u^*; u_1) f_1(t, u_*)\, f_1(t, u^*)\, \mathrm{d}u_*\, \mathrm{d}u^* \\ & - f_1(t, u_1) \int_{-\infty}^{+\infty} \eta_{11}(u_1, u^*)\, f_1(t, u^*)\, \mathrm{d}u^* \end{aligned} \tag{15}$$

$$\begin{aligned} Q_{12} \;=\; & \int_{-\infty}^{+\infty}\int_{-\infty}^{+\infty} \eta_{12}(u_*, u^*)\, A_{12}^{(1)}(u_*, u^*; u_1) f_1(t, u_*)\, f_2(t, u^*)\, \mathrm{d}u_*\, \mathrm{d}u^* \\ & - f_1(t, u_1) \int_{-\infty}^{+\infty} \eta_{12}(u_1, u^*)\, f_2(t, u^*)\, \mathrm{d}u^* \end{aligned} \tag{16}$$

$$\begin{aligned}\overline{Q}_1^{(r)} &= \int_{-\infty}^{+\infty}\int_{-\infty}^{+\infty} \eta_{11}^{(r)}(u_*,u^*)\,\tilde{A}_{11}^{(1)}(u_*,u^*;u_1)\,f_1(t,u_*)\,f_1(t,u^*)\,\mathrm{d}u_*\,\mathrm{d}u^* \\ &\quad -2f_1(t,u_1)\int_{-\infty}^{+\infty}\eta_{11}^{(r)}(u_1,u^*)\,f_1(t,u^*)\,\mathrm{d}u^* \\ &\quad +2\int_{-\infty}^{+\infty}\mathrm{d}u_*\int_{-\infty}^{+\infty}\eta_{21}^{(r)}(u_*,u^*)\,\tilde{A}_{21}^{(1)}(u_*,u^*;u_1)\,f_2(t,u_*)\,f_1(t,u^*)\,\mathrm{d}u^* \\ &\quad -f_1(t,u_1)\int_{-\infty}^{+\infty}\eta_{21}^{(r)}(u_1,u^*)\,f_2(t,u^*)\,\mathrm{d}u^* \end{aligned} \tag{17}$$

$$\begin{aligned}\overline{L}_1^{(r)} &= \int_{-\infty}^{+\infty}\mathrm{d}u_*\int_{-M}^{+M}\mu_2^{(r)}(u_*,v^*)\,B_2^{(1)}(u_*,v^*;u_1)\,f_2(t,u_*)\,\phi_2(v^*)\,\mathrm{d}v^* \\ &\quad -f_1(t,u_1)\int_{-M}^{+M}\mu_1^{(r)}(u_1,v^*)\,\phi_1(v^*)\,\mathrm{d}v^* \end{aligned} \tag{18}$$

Likewise, we can write for population 2:

$$\frac{\partial f_2}{\partial t}(t,u_2) = Q_{22} + Q_{21} + \overline{Q}_2^{(r)} + \overline{L}_2^{(r)} \tag{19}$$

where

$$\begin{aligned}Q_{22} &= \int_{-\infty}^{+\infty}\int_{-\infty}^{+\infty}\eta_{22}(u_*,u^*)\,A_{22}^{(2)}(u_*,u^*;u_2)\,f_2(t,u_*)\,f_2(t,u^*)\,\mathrm{d}u_*\,\mathrm{d}u^* \\ &\quad -f_2(t,u_2)\int_{-\infty}^{+\infty}\eta_{22}(u_2,u^*)\,f_2(t,u^*)\,\mathrm{d}u^* \end{aligned} \tag{20}$$

$$\begin{aligned}Q_{21} &= \int_{-\infty}^{+\infty}\int_{-\infty}^{+\infty}\eta_{21}(u_*,u^*)\,A_{21}^{(2)}(u_*,u^*;u_2)\,f_2(t,u_*)\,f_1(t,u^*)\,\mathrm{d}u_*\,\mathrm{d}u^* \\ &\quad -f_2(t,u_2)\int_{-\infty}^{+\infty}\eta_{21}(u_2,u^*)\,f_1(t,u^*)\,\mathrm{d}u^* \end{aligned} \tag{21}$$

$$\overline{Q}_2^{(r)} = \int_{-\infty}^{+\infty}\int_{-\infty}^{+\infty}\eta_{11}^{(r)}(u_*,u^*)\,\tilde{A}_{11}^{(2)}(u_*,u^*;u_2)\,f_1(t,u_*)\,f_1(t,u^*)\,\mathrm{d}u_*\,\mathrm{d}u^*$$

$$- f_2(t, u_2) \int_{-\infty}^{+\infty} \eta_{21}^{(r)}(u_2, u^*)\, f_1(t, u^*)\, \mathrm{d}u^* \tag{22}$$

$$\overline{L}_2^{(r)} = \int_{-\infty}^{+\infty} \mathrm{d}u_* \int_{-M}^{+M} \mu_1^{(r)}(u_*, v^*)\, B_1^{(2)}(u_*, v^*; u_2) f_1(t, u_*)\, \phi_1(v^*)\, \mathrm{d}v^*$$

$$- f_2(t, u_2) \int_{-M}^{+M} \mu_2^{(r)}(u_2, v^*)\, \phi_2(v^*)\, \mathrm{d}v^*. \tag{23}$$

In the above equations, η_{hk} (and $\eta_{hk}^{(r)}$) is called encounter rate and it describes the rate of interactions (that is, the number of encounters per unit time) between individuals of the h-th population and individuals of the k-th population, while $\mu_h^{(r)}$ refers to the rate of interaction between individuals of the h-th population and the immune system. To construct the transition rates, we assume that the interactions between individuals can be modeled in analogy to the intermolecular potentials acting between the gas molecules. Since in the framework of kinetic theory of rarefied gases analytical manipulations can be carried out in closed form for Maxwell molecules (see Appendix) (Cercignani 1988), we restrict ourselves to this kind of interaction, which leads to assume η_{hk} constant. In particular, when the encounters between individuals belonging to different groups are forbidden, in the framework of our epidemiological model, the rates η_{hk} vanish. Thus, for the operator Q_{11}, since all types of interactions between healthy and positive asymptomatic people are allowed, we set

$$\eta_{11}(u_*, u^*) = \bar{\eta}_{11} \qquad \forall\, u_* \in \mathbb{R}, \quad u^* \in \mathbb{R}.$$

In the operator Q_{22}, since positive symptomatic individuals cannot interact with hospitalized people, we have

$$\eta_{22}(u_*, u^*) = \begin{cases} \bar{\eta}_{22} & \text{if } (u_* < 0, u^* < 0) \text{ or } (u_* > 0, u^* > 0) \\ 0 & \text{otherwise} \end{cases}$$

The interactions between the two populations 1 and 2 describe only the possible contacts between the ill individuals and the medical staff (healthy); therefore,

$$\eta_{12}(u_*, u^*) = \begin{cases} \bar{\eta}_{12} & \text{if } u_* < 0 \quad \text{in } f_1(t, u_*) \\ 0 & \text{otherwise} \end{cases}$$

$$\eta_{21}(u_*, u^*) = \begin{cases} \bar{\eta}_{21} & \text{if } u^* < 0 \quad \text{in } f_1(t, u^*) \\ 0 & \text{otherwise} \end{cases}$$

and moreover, since both rates refer to the same type of interactions, we assume

$$\bar{\eta}_{12} = \bar{\eta}_{21}.$$

For the switch $1 + 1 \to 2 + 1$ that can occur when two positive asymptomatic individuals interact, we set

$$\eta_{11}^{(r)}(u_*, u^*) = \begin{cases} \bar{\eta}_{11}^{(r)} & \text{if } u_* > 0 \text{ and } u^* > 0 \\ 0 & \text{otherwise} \end{cases}$$

For the reverse switch $2 + 1 \to 1 + 1$, taking into account that population 2 may interact only with the medical staff, we have

$$\eta_{21}^{(r)}(u_*, u^*) = \begin{cases} \bar{\eta}_{21}^{(r)} & \text{if } u^* < 0 \quad \text{in } f_1(t, u^*) \\ 0 & \text{otherwise} \end{cases}$$

It is worth noting that the rates of interactions $\bar{\eta}_{12}$ and $\bar{\eta}_{21}^{(r)}$ have to take into account the probability for sick people to find available doctors and, concerning $\bar{\eta}_{21}^{(r)}$, also the probability of recovery, depending both on the available medical staff and on the severity of the disease. For this reason, a more realistic version of this mathematical model (but not easily manageable from the analytical point of view) should take $\bar{\eta}_{21}^{(r)}$ explicitly dependent on the viral load u_* of the ill interacting individual.

The interactions with the immune system involve the positive asymptomatic persons in population 1 and all the individuals in population 2; for this reason, we set

$$\mu_1^{(r)}(u_*, v^*) = \begin{cases} \bar{\mu}_1^{(r)} & \text{if } u_* > 0 \quad \text{in } f_1(t, u_*) \\ 0 & \text{otherwise} \end{cases}$$

and

$$\mu_2^{(r)}(u_*, v^*) = \bar{\mu}_2^{(r)} \qquad \forall\, u_* \in \mathbb{R}, \quad v^* \in [-M, M]$$

The modification of the state of interacting individuals is described by the transition probability density, $A_{hk}^{(i)}(u_*, u^*; u_i)$, of individuals which are shifted into the i-th population with state u_i due to encounters between an individual of the h-th population in the state u_* with an individual of the k-th population in the state u^*. Likewise, $B_h^{(i)}(u_*, v^*; u_i)$ represents the transition probability density of individuals which are shifted into the i-th population with state u_i due to the interaction between an individual of the h-th population in the state u_* with the immune system characterized by the microscopic state v^*. The products $\eta_{hk}\, A_{hk}^{(i)}$ and $\mu_h^{(r)}\, B_h^{(i)}$ give the transition rates.

For stochastic models of interaction between individuals, the transition probability density $A_{hk}^{(i)}$ satisfies the following properties:

(i)

$$A_{hk}^{(i)}(u_*, u^*; u_i) = A_{kh}^{(i)}(u^*, u_*; u_i) \tag{24}$$

expressing indistinguishability of individuals;

(ii)

$$\int_{-\infty}^{+\infty} \mathrm{d}u_i \, A_{hk}^{(i)}(u_*, u^*; u_i) = 1 \qquad \forall h, k. \tag{25}$$

We assume that also the probability density $B_h^{(i)}$ is normalized with respect to all possible final states:

$$\int_{-\infty}^{+\infty} \mathrm{d}u_i \, B_h^{(i)}(u_*, v^*; u_i) = 1 \qquad \forall h. \tag{26}$$

Stochastic models, describing the interactions within each population, have been proposed in order to give an explicit expression for the transition probabilities $A_{hk}^{(i)}$ and $B_h^{(i)}$ in the interaction operators of the Boltzmann equations (Eqs. 14 and 19).

In particular, the interactions within the population 1, taken into account by the term Q_{11}, can be modeled as follows: If the interacting individuals are both healthy (with microscopic states $u_*, u^* < 0$) or both positive asymptomatic (with $u_*, u^* > 0$), one has

$$\begin{cases} u_*' = u_* \\ u'^* = u^*, \end{cases} \tag{27}$$

while if a healthy individual (with $u_* < 0$) interacts with a positive asymptomatic (with $u^* > 0$), the output is

$$\begin{cases} u_*' = (1-\theta)u_* + \theta u^* \\ u'^* = (1-\theta)u_* + \theta u^* \end{cases} \tag{28}$$

where θ denotes a Bernoulli random variable taking the value $\theta = 1$ with probability $\beta \in [0, 1]$ and the value $\theta = 0$ with probability $1 - \beta$. Consequently, the expected value of both post-interaction states u_*' and u'^* is

$$\begin{aligned} E_\theta[u_*'] &= (u_*')_{|\theta=0}\mathrm{Prob}(\theta = 0) + (u_*')_{|\theta=1}\mathrm{Prob}(\theta = 1) = (1-\beta)u_* + \beta\, u^* \\ E_\theta[u'^*] &= (u'^*)_{|\theta=0}\mathrm{Prob}(\theta = 0) + (u'^*)_{|\theta=1}\mathrm{Prob}(\theta = 1) = (1-\beta)u_* + \beta\, u^* \end{aligned} \tag{29}$$

Thus, the parameter β represents the contagious index of the disease: the limiting option $\beta = 1$ describes an extremely contagious disease (pandemic), in which each healthy individual interacting with a positive asymptomatic becomes infectious, and a positive asymptomatic individual never recovers in these interactions; the other limit $\beta = 0$ corresponds to a situation in which a healthy individual cannot become infectious and the positive asymptomatic persons immediately recover; therefore, no pandemic is ongoing. The intermediate value $\beta = 1/2$ provides $E_\theta[u_*'] = E_\theta[u'^*] =$

$\frac{1}{2}(u_* + u^*)$; therefore, the probability for a healthy individual to get sick equals the probability for an asymptomatic person to recover, and this implies (as it will be proved below) that the total number of healthy and positive asymptomatic individuals does not change.

Concerning the interactions described by the operator Q_{12}, only a doctor (healthy, with $u_* < 0$) can interact with people of population 2 (with state $u^* \in \mathbb{R}$), providing

$$\begin{cases} u'_* = u_* \\ u'^* = u^*. \end{cases} \tag{30}$$

As regards the rules underlying the transition probabilities in the term Q_{22}, interactions between hospitalized people do not cause changes ($u'_* = u_*$ and $u'^* = u^*$), while an interaction between two positive symptomatic leads to a possible aggravation of the status of one of them, described through a Bernoulli variable θ such that if $\theta = 1$ the status does not change while if $\theta = 0$, the status changes sign and the individual becomes hospitalized. Post-interaction states are thus provided by

$$\begin{cases} u'_* = \theta u_* + (1-\theta)(-u^*) \\ u'^* = u^* \end{cases} \tag{31}$$

and, denoting with $\alpha \in [0, 1]$ the probability that $\theta = 1$, the expected post-interaction state is

$$E_\theta[u'_*] = (u'_*)_{|\theta=0}\text{Prob}(\theta = 0) + (u'_*)_{|\theta=1}\text{Prob}(\theta = 1) = \alpha\, u_* + (1-\alpha)\,(-u^*).$$

Furthermore, encounters between individuals which generate a population transition can be modeled as follows:

(a) interaction rule for the direct transition $1 + 1 \to 2 + 1$ with states $(u^* > 0, u_* > 0) \to (u'^* < 0, u'_* > 0)$, respectively:

$$\begin{cases} u'_* = u_* \\ u'^* = -u^* \end{cases} \tag{32}$$

thus, an asymptomatic individual becomes symptomatic;

(b) interaction rule for the reverse transition $2 + 1 \to 1 + 1$ with states $(u^* \in \mathbb{R}, u_* < 0) \to (u'^* < 0, u'_* < 0)$, respectively, in which an ill individual recovers due to interactions with medical staff:

$$\begin{cases} u'_* = u_* \\ u'^* = u_* \end{cases} \tag{33}$$

Finally, we describe the interactions of the individuals with the immune system as follows:

(a) interaction rules with the innate immune system described by the distribution function ϕ_1, where some asymptomatic individuals ($u_* > 0$) pass to population 2

becoming symptomatic ($u'_* < 0$):

$$\begin{cases} u'_* = -u_* \\ v'^* = v^* \end{cases} \tag{34}$$

(b) interaction rules with the adaptive immune system, modeled by the distribution function ϕ_2, leading people of population 2 to recover:

$$\begin{cases} u'_* = -|u_*| \\ v'^* = v^* \end{cases} \tag{35}$$

The average action of the immune system on asymptomatic individuals is described by

$$\hat{I}_1 = \int_{-M}^{+M} \phi_1(v)\,\mathrm{d}v \tag{36}$$

while the action on the ill people is accounted for by

$$\hat{I}_2 = \int_{-M}^{+M} \phi_2(v)\,\mathrm{d}v. \tag{37}$$

The term $(\bar{\mu}_1^{(r)}\hat{I}_1)$ takes very large values when the innate immune cells of an initially positive asymptomatic person (who has already contracted the virus) trigger an exacerbated inflammatory response (hyperinflammation) leading to a major complication of Covid-19. Therefore, in this case, a significant fraction of asymptomatic people become ill and a transition to population 2 occurs. On the contrary, a strong response of the adaptive immune system (that is, a large value of the term $(\bar{\mu}_2^{(r)}\hat{I}_2)$) allows an individual, belonging to population 2, to recover without specific treatments. In fact, adaptive immunity encompasses a set of specific protective mechanisms against certain pathogens. Adaptive immunity can also be acquired through the administration of vaccines, which in turn increase the anti-viral activity of some innate immune cells (Zhu et al. 2022). Therefore, the impact of vaccination can be taken into account in our model by increasing the term $(\bar{\mu}_2^{(r)}\hat{I}_2)$ and, at the same time, decreasing $(\bar{\mu}_1^{(r)}\hat{I}_1)$. Moreover, explicitly modeling the action of the immune system allows us to account for individuals of different ages since older people (with a weaker immune system) get sick more easily with a higher probability of an unfavorable outcome of the disease.

By taking into account the interaction rules presented above, the transition probability densities $A_{hk}^{(i)}$ and $B_h^{(i)}$ can be explicitly written.

(1) For the operator Q_{11}, we can distinguish between the following cases:

(i)

$$A_{11}^{(1)}(u_* < 0, u^* < 0; u_1) = \delta(u_1 - u_*) \tag{38}$$

(ii)

$$A_{11}^{(1)}(u_* > 0, u^* < 0; u_1) = \beta\,\delta(u_1 - u_*) + (1-\beta)\,\delta(u_1 - u^*) \tag{39}$$

where $\beta \in [0, 1]$. The value assumed by β allows us to take into account different variants of the main virus characterized by different transmission levels. In fact, as already remarked above, the value $\beta = 1$ indicates a highly contagious variant since all healthy individuals, which interact with positive asymptomatic persons, change their category. On the contrary, when $\beta = 0$, there is no spread of the contagious disease, since one has the recovery of all asymptomatic individuals.

(iii)

$$A_{11}^{(1)}(u_* > 0, u^* > 0; u_1) = \delta(u_1 - u_*). \tag{40}$$

(2) For the operator Q_{12}, we have:

$$A_{12}^{(1)}(u_* < 0, u^* \in \mathbb{R}; u_1) = \delta(u_1 - u_*) \tag{41}$$

with $A_{12}^{(1)} = A_{21}^{(2)}$.

(3) For the operator Q_{22}, we can distinguish between the following cases:

(i)

$$A_{22}^{(2)}(u_* > 0, u^* > 0; u_2) = \delta(u_2 - u_*) \tag{42}$$

(ii)

$$A_{22}^{(2)}(u_* < 0, u^* < 0; u_2) = \alpha\,\delta(u_2 - u_*) + (1-\alpha)\,\delta(u_2 + u^*) \tag{43}$$

where $\alpha \in [0, 1]$. If $\alpha = 1$, the positive symptomatic individuals remain in the same infectious state, while if $\alpha = 0$, they are exposed to a worsening of their disease and become hospitalized.

(4) Encounters between individuals which generate a population transition, described by the switch Boltzmann operator $\overline{Q}_1^{(r)}$, give rise to the following transition probability densities:

(i)

$$\tilde{A}_{11}^{(1)}(u_* > 0, u^* > 0; u_1) = \delta(u_1 - u_*) \tag{44}$$

(ii)

$$\tilde{A}_{21}^{(1)}(u_* \in \mathbb{R}, u^* < 0; u_1) = \delta(u_1 - u^*) \tag{45}$$

while encounters described by the switch operator $\overline{Q}_2^{(r)}$ give:

(iii)

$$\tilde{A}_{11}^{(2)}(u_* > 0, u^* > 0; u_2) = \delta(u_2 + u_*). \tag{46}$$

To conclude, the transition probability density $B_1^{(2)}(u_* > 0, v^*; u_2)$ of individuals which are shifted into population 2, with the state $u_2 < 0$, due to the interaction between an individual of population 1, in the state $u_* > 0$, with the innate immune system, appearing in the term $\overline{L}_2^{(r)}$, is given by

$$B_1^{(2)}(u_* > 0, v^*; u_2) = \delta(u_2 + u_*). \tag{47}$$

Furthermore, the transition probability density $B_2^{(1)}(u_* \in \mathbb{R}, v^*; u_1)$ of individuals which are shifted into population 1, with the state $u_1 < 0$, due to the interaction between an individual of population 2 in the state $u_* \in \mathbb{R}$ with the adaptive immune system, appearing in the term $\overline{L}_1^{(r)}$, is given by

$$B_2^{(1)}(u_* \in \mathbb{R}, v^*; u_1) = \delta(u_1 + |u_*|). \tag{48}$$

Since this last interaction allows a complete recovery of positive symptomatic or hospitalized individuals ($u_1 \in [-\infty, 0[$), the following relation holds:

$$\int_{-\infty}^{0} \mathrm{d}u_1 \, B_2^{(1)}(u_*, v^*; u_1) = 1. \tag{49}$$

Global existence and uniqueness of the solutions to the Boltzmann-type equations, based on the scattering kernel formulation of the collision operator, have been proven in De Lillo et al. (2009).

3 Evolution Equations for the Size of Each Population

In order to derive the macroscopic equations for the evolution of the size of the two populations, we have to integrate Eq. (14) with respect to u_1 and Eq. (19) with respect to u_2. Taking into account that interactions without switches do not give any contribution (since they do not change the number of individuals of populations 1 and 2), we get

$$\frac{\mathrm{d}n_1}{\mathrm{d}t} = \int_{-\infty}^{+\infty} \overline{Q}_1^{(r)}(u_1)\,\mathrm{d}u_1 + \int_{-\infty}^{+\infty} \overline{L}_1^{(r)}(u_1)\,\mathrm{d}u_1, \tag{50}$$

$$\frac{\mathrm{d}n_2}{\mathrm{d}t} = \int_{-\infty}^{+\infty} \overline{Q}_2^{(r)}(u_2)\,\mathrm{d}u_2 + \int_{-\infty}^{+\infty} \overline{L}_2^{(r)}(u_2)\,\mathrm{d}u_2. \tag{51}$$

Bearing in mind the definitions of the interaction rates $\eta_{hk}^{(r)}$, $\mu_h^{(r)}$ and the transition probability densities $A_{hk}^{(i)}$, $B_h^{(i)}$ given above, the equations read:

$$\frac{\mathrm{d}n_1}{\mathrm{d}t} = -\bar{\eta}_{11}^{(r)}\,(n_1^A)^2 + \bar{\eta}_{21}^{(r)}\,n_2\,n_1^{HE} + \bar{\mu}_2^{(r)}\,n_2\,\hat{I}_2 - \bar{\mu}_1^{(r)}\,n_1^A\,\hat{I}_1 \tag{52}$$

$$\frac{\mathrm{d}n_2}{\mathrm{d}t} = \bar{\eta}_{11}^{(r)}\,(n_1^A)^2 - \bar{\eta}_{21}^{(r)}\,n_2\,n_1^{HE} - \bar{\mu}_2^{(r)}\,n_2\,\hat{I}_2 + \bar{\mu}_1^{(r)}\,n_1^A\,\hat{I}_1 \tag{53}$$

In order to find a closed system of equations, let us rewrite the terms on the right-hand side of Eq. (14) as follows, taking into account the interaction rules (38)–(48).

$$\begin{aligned}
Q_{11} &= \overline{\eta}_{11}\int_{-\infty}^{+\infty}\mathrm{d}u_*\,f_1(t,u_*)\Big\{\int_{-\infty}^{0}A_{11}^{(1)}(u_*,u^*;u_1)\,f_1(t,u^*)\,\mathrm{d}u^*\\
&\quad+\int_{0}^{+\infty}A_{11}^{(1)}(u_*,u^*;u_1)\,f_1(t,u^*)\,\mathrm{d}u^*\Big\}\\
&\quad-\overline{\eta}_{11}\,f_1(t,u_1)\Big\{\int_{-\infty}^{0}f_1(t,u^*)\,\mathrm{d}u^*+\int_{0}^{+\infty}f_1(t,u^*)\,\mathrm{d}u^*\Big\}\\
&=\overline{\eta}_{11}\Big\{\int_{-\infty}^{0}\mathrm{d}u_*\,f_1(t,u_*)+\int_{0}^{+\infty}\mathrm{d}u_*\,f_1(t,u_*)\Big\}\cdot\int_{-\infty}^{0}A_{11}^{(1)}(u_*,u^*;u_1)\,f_1(t,u^*)\,\mathrm{d}u^*\\
&\quad+\overline{\eta}_{11}\Big\{\int_{-\infty}^{0}\mathrm{d}u_*\,f_1(t,u_*)+\int_{0}^{+\infty}\mathrm{d}u_*\,f_1(t,u_*)\Big\}\cdot\int_{0}^{+\infty}A_{11}^{(1)}(u_*,u^*;u_1)\,f_1(t,u^*)\,\mathrm{d}u^*\\
&\quad-\overline{\eta}_{11}f_1(t,u_1)\int_{-\infty}^{0}\mathrm{d}u^*\,f_1(t,u^*)-\overline{\eta}_{11}f_1(t,u_1)\int_{0}^{+\infty}\mathrm{d}u^*\,f_1(t,u^*)\\
&=\overline{\eta}_{11}\int_{-\infty}^{0}\mathrm{d}u_*\,f_1(t,u_*)\int_{-\infty}^{0}A_{11}^{(1)}(u_*,u^*;u_1)\,f_1(t,u^*)\,\mathrm{d}u^*\\
&\quad+2\,\overline{\eta}_{11}\int_{0}^{+\infty}\mathrm{d}u_*\,f_1(t,u_*)\int_{-\infty}^{0}A_{11}^{(1)}(u_*,u^*;u_1)\,f_1(t,u^*)\,\mathrm{d}u^*\\
&\quad+\overline{\eta}_{11}\int_{0}^{+\infty}\mathrm{d}u_*\,f_1(t,u_*)\int_{0}^{+\infty}A_{11}^{(1)}(u_*,u^*;u_1)\,f_1(t,u^*)\,\mathrm{d}u^*\\
&\quad-\overline{\eta}_{11}f_1(t,u_1)\int_{-\infty}^{0}f_1(t,u^*)\,\mathrm{d}u^*-\overline{\eta}_{11}f_1(t,u_1)\int_{0}^{+\infty}\mathrm{d}u^*\,f_1(t,u^*)\\
&=\overline{\eta}_{11}f_1(t,u_1<0)\int_{-\infty}^{0}\mathrm{d}u^*\,f_1(t,u^*)+2\overline{\eta}_{11}\,\beta\,f_1(t,u_1>0)\int_{-\infty}^{0}\mathrm{d}u^*\,f_1(t,u^*)
\end{aligned}$$

$$+2\overline{\eta}_{11}\,(1-\beta)\,f_1(t,u_1<0)\int_0^{+\infty}\mathrm{d}u_*\,f_1(t,u_*)+\overline{\eta}_{11}f_1(t,u_1>0)\int_0^{+\infty}\mathrm{d}u^*\,f_1(t,u^*)$$

$$-\overline{\eta}_{11}f_1(t,u_1)\int_{-\infty}^{0}\mathrm{d}u^*\,f_1(t,u^*)-\overline{\eta}_{11}f_1(t,u_1)\int_0^{+\infty}\mathrm{d}u^*\,f_1(t,u^*) \tag{54}$$

$$Q_{12}=\overline{\eta}_{12}\int_{-\infty}^{0}\mathrm{d}u_*\,f_1(t,u_*)\int_{-\infty}^{+\infty}A_{12}^{(1)}(u_*,u^*;u_1)\,f_2(t,u^*)\,\mathrm{d}u^*$$

$$-\overline{\eta}_{12}\,f_1(t,u_1<0)\int_{-\infty}^{+\infty}f_2(t,u^*)\,\mathrm{d}u^*$$

$$=\overline{\eta}_{12}\,f_1(t,u_1<0)\int_{-\infty}^{+\infty}f_2(t,u^*)\,\mathrm{d}u^*-\overline{\eta}_{12}\,f_1(t,u_1<0)\int_{-\infty}^{+\infty}f_2(t,u^*)\,\mathrm{d}u^*=0 \tag{55}$$

$$\overline{Q}_1^{(r)}=\overline{\eta}_{11}^{(r)}\int_0^{+\infty}\int_0^{+\infty}\tilde{A}_{11}^{(1)}(u_*,u^*;u_1)\,f_1(t,u_*)\,f_1(t,u^*)\,\mathrm{d}u_*\,\mathrm{d}u^*$$

$$-2\overline{\eta}_{11}^{(r)}\,f_1(t,u_1>0)\int_0^{+\infty}f_1(t,u^*)\,\mathrm{d}u^*$$

$$+2\overline{\eta}_{21}^{(r)}\int_{-\infty}^{0}\mathrm{d}u^*\,f_1(t,u^*)\int_{-\infty}^{+\infty}\tilde{A}_{21}^{(1)}(u_*,u^*;u_1)\,f_2(t,u_*)\,\mathrm{d}u_*$$

$$-\overline{\eta}_{21}^{(r)}\,f_1(t,u_1<0)\int_{-\infty}^{+\infty}f_2(t,u^*)\,\mathrm{d}u^*$$

$$=-\overline{\eta}_{11}^{(r)}\,f_1(t,u_1>0)\int_0^{+\infty}f_1(t,u^*)\,\mathrm{d}u^*+\overline{\eta}_{21}^{(r)}\,f_1(t,u_1<0)\int_{-\infty}^{+\infty}f_2(t,u_*)\,\mathrm{d}u_*$$

$$\overline{L}_1^{(r)}=\overline{\mu}_2^{(r)}\int_{-\infty}^{+\infty}\mathrm{d}u_*\int_{-M}^{+M}B_2^{(1)}(u_*,v^*;u_1)\,f_2(t,u_*)\,\phi_2(v^*)\,\mathrm{d}v^*$$

$$-\overline{\mu}_1^{(r)}\,f_1(t,u_1>0)\int_{-M}^{+M}\phi_1(v^*)\,\mathrm{d}v^* \tag{56}$$

Integrating Eq. (14) first with respect to $u_1\in(-\infty,0)$ and then with respect to $u_1\in(0,+\infty)$, one obtains

$$\frac{\mathrm{d}n_1^{HE}}{\mathrm{d}t}=(1-2\,\beta)\,\overline{\eta}_{11}\,n_1^{HE}\,n_1^A+\overline{\eta}_{21}^{(r)}\,n_1^{HE}\,n_2+\overline{\mu}_2^{(r)}\,\hat{I}_2\,n_2 \tag{57}$$

$$\frac{\mathrm{d}n_1^A}{\mathrm{d}t} = (2\,\beta - 1)\overline{\eta}_{11}\, n_1^{HE}\, n_1^A - \overline{\eta}_{11}^{(r)}\,(n_1^A)^2 - \overline{\mu}_1^{(r)}\,\hat{I}_1\, n_1^A \tag{58}$$

The expressions (57), (58) and (53) form a closed system of equations that can be solved to give the time evolution of the size of the populations n_1^{HE}, n_1^A, n_2.

In order to investigate separately the time evolution of n_2^S and n_2^{HS}, analogous computations as those reported above can be performed starting from Eq. (19). Rewriting the terms on the right-hand side as follows:

$$\begin{aligned}
Q_{22} =& \overline{\eta}_{22} \int_{-\infty}^{0}\int_{-\infty}^{0} A_{22}^{(2)}(u_*, u^*; u_2)\, f_2(t, u_*)\, f_2(t, u^*)\,\mathrm{d}u_*\,\mathrm{d}u^* \\
&+ \overline{\eta}_{22} \int_{0}^{+\infty}\int_{0}^{+\infty} A_{22}^{(2)}(u_*, u^*; u_2)\, f_2(t, u_*)\, f_2(t, u^*)\,\mathrm{d}u_*\,\mathrm{d}u^* \\
&- \overline{\eta}_{22}\, f_2(t, u_2 < 0) \int_{-\infty}^{0} f_2(t, u^*)\,\mathrm{d}u^* - \overline{\eta}_{22}\, f_2(t, u_2 > 0) \int_{0}^{+\infty} f_2(t, u^*)\,\mathrm{d}u^* \\
=& \overline{\eta}_{22}\,\alpha\, f_2(t, u_2 < 0) \int_{-\infty}^{0} f_2(t, u^*)\,\mathrm{d}u^* \\
&+ \overline{\eta}_{22}\,(1-\alpha) \int_{-\infty}^{0}\int_{-\infty}^{0} \delta(u_2 + u_*)\, f_2(t, u_*)\, f_2(t, u^*)\,\mathrm{d}u_*\,\mathrm{d}u^* \\
&- \overline{\eta}_{22}\, f_2(t, u_2 < 0) \int_{-\infty}^{0} f_2(t, u^*)\,\mathrm{d}u^*
\end{aligned} \tag{59}$$

$$\begin{aligned}
Q_{21} =& \overline{\eta}_{21} \int_{-\infty}^{0} \mathrm{d}u^*\, f_1(t, u^*) \int_{-\infty}^{+\infty} A_{21}^{(2)}(u_*, u^*; u_2)\, f_2(t, u_*)\,\mathrm{d}u_* \\
&- \overline{\eta}_{21}\, f_2(t, u_2) \int_{-\infty}^{0} f_1(t, u^*)\,\mathrm{d}u^* \\
=& \overline{\eta}_{21}\, f_2(t, u_2) \int_{-\infty}^{0} f_1(t, u^*)\,\mathrm{d}u^* - \overline{\eta}_{21}\, f_2(t, u_2) \int_{-\infty}^{0} f_1(t, u^*)\,\mathrm{d}u^* = 0
\end{aligned} \tag{60}$$

$$\overline{Q}_2^{(r)} = \overline{\eta}_{11}^{(r)} \int_{0}^{+\infty}\int_{0}^{+\infty} \tilde{A}_{11}^{(2)}(u_*, u^*; u_2)\, f_1(t, u_*)\, f_1(t, u^*)\,\mathrm{d}u_*\,\mathrm{d}u^*$$

$$
\begin{aligned}
&- \overline{\eta}_{21}^{(r)}\, f_2(t,u_2) \int_{-\infty}^{0} f_1(t,u^*)\,\mathrm{d}u^* \\
&= \overline{\eta}_{11}^{(r)} \int_0^{+\infty}\int_0^{+\infty} \delta(u_2+u_*)\, f_1(t,u_*)\, f_1(t,u^*)\,\mathrm{d}u_*\,\mathrm{d}u^* \\
&\quad - \overline{\eta}_{21}^{(r)}\, f_2(t,u_2) \int_{-\infty}^{0} f_1(t,u^*)\,\mathrm{d}u^* \qquad (61)\\
\overline{L}_2^{(r)} &= \overline{\mu}_1^{(r)} \int_0^{+\infty} \mathrm{d}u_* \int_{-M}^{+M} B_1^{(2)}(u_*,v^*;u_2)\, f_1(t,u_*)\,\phi_1(v^*)\,\mathrm{d}v^* \\
&\quad - \overline{\mu}_2^{(r)}\, f_2(t,u_2) \int_{-M}^{+M} \phi_2(v^*)\,\mathrm{d}v^* \qquad (62)
\end{aligned}
$$

and integrating Eq. (19) first with respect to $u_2 \in (-\infty, 0)$ and then with respect to $u_2 \in (0, +\infty)$, we get

$$
\frac{\mathrm{d}n_2^S}{\mathrm{d}t} = -(1-\alpha)\,\overline{\eta}_{22}\,(n_2^S)^2 + \overline{\eta}_{11}^{(r)}\,(n_1^A)^2 - \overline{\eta}_{21}^{(r)}\,n_1^{HE}\,n_2^S - \overline{\mu}_2^{(r)}\,\hat{I}_2\,n_2^S + \overline{\mu}_1^{(r)}\,\hat{I}_1\,n_1^A \qquad (63)
$$

$$
\frac{\mathrm{d}n_2^{HS}}{\mathrm{d}t} = (1-\alpha)\,\overline{\eta}_{22}\,(n_2^S)^2 - \overline{\eta}_{21}^{(r)}\,n_1^{HE}\,n_2^{HS} - \overline{\mu}_2^{(r)}\,\hat{I}_2\,n_2^{HS} \qquad (64)
$$

The sum of Eqs. (63) and (64) correctly reproduces Eq. (53) for the total density n_2.

Usually, in epidemiological models, the so-called basic reproduction number (R_0), which describes the dynamics of the infectious class, is defined in order to quantify the contagiousness or transmissibility of a virus. The larger the value of R_0, the harder it is to control the spread of an infectious disease. R_0 is rarely measured directly, and its values, deduced from mathematical models, depend critically on the model structure, the initial conditions, and several other modeling assumptions (Hethcote 2000). In the framework of the present analysis, we propose the following definition of time-dependent effective reproduction number:

$$
R_0(t) = \frac{\overline{\eta}_{11}^{(r)}\,(n_1^A)^2 + \overline{\mu}_1^{(r)}\,n_1^A\,\hat{I}_1}{\overline{\eta}_{21}^{(r)}\,n_2\,n_1^{HE} + \overline{\mu}_2^{(r)}\,n_2\,\hat{I}_2} \qquad (65)
$$

which characterizes the change in the number of the infected individuals belonging to population 2 (see Eq. (53)) "Albi et al. (2022)". In Sect. 7, we assess the reliability of such a definition (65) as control parameter of the epidemic.

4 Evolution Equations for the Mean State of Each Population

We derive from the Boltzmann model presented in Sect. 2 the evolution equations for the total values of the internal states

$$U_1^{HE} = \int_{-\infty}^{0} u_1\, f_1(t,u_1)\,\mathrm{d}u_1, \qquad U_1^{A} = \int_{0}^{+\infty} u_1\, f_1(t,u_1)\,\mathrm{d}u_1,$$
$$U_2^{S} = \int_{-\infty}^{0} u_2\, f_2(t,u_2)\,\mathrm{d}u_2, \qquad U_2^{HS} = \int_{0}^{+\infty} u_2\, f_2(t,u_2)\,\mathrm{d}u_2$$

where the superscripts have the same meaning as those appearing in formulas (5)–(8). The equation for U_1^{HE} is provided by

$$\frac{\mathrm{d}U_1^{HE}}{\mathrm{d}t} = \int_{-\infty}^{0} u_1\Big[Q_{11} + Q_{12} + \overline{Q}_1^{(r)} + \overline{L}_1^{(r)}\Big]\mathrm{d}u_1, \tag{66}$$

and since

$$\int_{-\infty}^{0} u_1\, Q_{11}\,\mathrm{d}u_1 = -(2\beta-1)\bar{\eta}_{11}U_1^{HE}\,n_1^A, \qquad \int_{-\infty}^{0} u_1\, Q_{12}\,\mathrm{d}u_1 = 0,$$
$$\int_{-\infty}^{0} u_1\,\overline{Q}_1^{(r)}\,\mathrm{d}u_1 = \bar{\eta}_{21}^{(r)}U_1^{HE}n_2, \qquad \int_{-\infty}^{0} u_1\,\overline{L}_1^{(r)}\,\mathrm{d}u_1 = \bar{\mu}_2^{(r)}\hat{I}_2(U_2^S - U_2^{HS}),$$

it turns out to be

$$\frac{\mathrm{d}U_1^{HE}}{\mathrm{d}t} = -(2\beta-1)\bar{\eta}_{11}U_1^{HE}\,n_1^A + \bar{\eta}_{21}^{(r)}U_1^{HE}\,n_2 + \bar{\mu}_2^{(r)}\,\hat{I}_2\,(U_2^S - U_2^{HS}). \tag{67}$$

Analogously, the equation for U_1^A reads

$$\frac{\mathrm{d}U_1^{A}}{\mathrm{d}t} = \int_{0}^{+\infty} u_1\Big[Q_{11} + Q_{12} + \overline{Q}_1^{(r)} + \overline{L}_1^{(r)}\Big]\mathrm{d}u_1, \tag{68}$$

and since

$$\int_0^{+\infty} u_1\, Q_{11}\, \mathrm{d}u_1 = (2\,\beta - 1)\bar{\eta}_{11} U_1^A n_1^{HE}, \qquad \int_0^{+\infty} u_1\, Q_{12}\, \mathrm{d}u_1 = 0,$$

$$\int_0^{+\infty} u_1\, \overline{Q}_1^{(r)}\, \mathrm{d}u_1 = -\,\bar{\eta}_{11}^{(r)} U_1^A n_1^A, \qquad \int_0^{+\infty} u_1\, \overline{L}_1^{(r)}\, \mathrm{d}u_1 = -\,\bar{\mu}_1^{(r)} U_1^A \hat{I}_1,$$

we get

$$\frac{\mathrm{d}U_1^A}{\mathrm{d}t} = (2\,\beta - 1)\bar{\eta}_{11} U_1^A n_1^{HE} - \bar{\eta}_{11}^{(r)} U_1^A n_1^A - \bar{\mu}_1^{(r)} U_1^A \hat{I}_1. \tag{69}$$

On the same ground, we can derive the evolution equations for U_2^S and U_2^{HS}. Taking into account the following expressions: On the same ground, we

$$\int_{-\infty}^{0} u_2\, Q_{22}\, \mathrm{d}u_2 = -(1-\alpha)\bar{\eta}_{22} U_2^S\, n_2^S,$$

$$\int_{-\infty}^{0} u_2\, Q_{21}\, \mathrm{d}u_2 = 0,$$

$$\int_{-\infty}^{0} u_2\, \overline{Q}_2^{(r)}\, \mathrm{d}u_2 = -\bar{\eta}_{11}^{(r)} U_1^A n_1^A - \bar{\eta}_{21}^{(r)} U_2^S n_1^{HE},$$

$$\int_{-\infty}^{0} u_2\, \overline{L}_2^{(r)}\, \mathrm{d}u_2 = -\bar{\mu}_1^{(r)} U_1^A \hat{I}_1 - \bar{\mu}_2^{(r)} U_2^S \hat{I}_2,$$

and

$$\int_0^{+\infty} u_2\, Q_{22}\, \mathrm{d}u_2 = -(1-\alpha)\bar{\eta}_{22} U_2^S n_2^S, \qquad \int_0^{+\infty} u_2\, Q_{21}\, \mathrm{d}u_2 = 0,$$

$$\int_0^{+\infty} u_2\, \overline{Q}_2^{(r)}\, \mathrm{d}u_2 = -\,\bar{\eta}_{21}^{(r)} U_2^{HS} n_1^{HE}, \qquad \int_0^{+\infty} u_2\, \overline{L}_2^{(r)}\, \mathrm{d}u_2 = -\,\bar{\mu}_2^{(r)} U_2^{HS} \hat{I}_2$$

we obtain

$$\frac{\mathrm{d}U_2^S}{\mathrm{d}t} = -\,(1-\alpha)\,\bar{\eta}_{22} U_2^S\, n_2^S - \bar{\eta}_{11}^{(r)} U_1^A\, n_1^A - \bar{\eta}_{21}^{(r)} U_2^S\, n_1^{HE} - \bar{\mu}_1^{(r)}\, \hat{I}_1\, U_1^A - \bar{\mu}_2^{(r)}\, \hat{I}_2\, U_2^S \tag{70}$$

$$\frac{\mathrm{d}U_2^{HS}}{\mathrm{d}t} = -\,(1-\alpha)\,\bar{\eta}_{22} U_2^S\, n_2^S - \bar{\eta}_{21}^{(r)} U_2^{HS}\, n_1^{HE} - \bar{\mu}_2^{(r)}\, \hat{I}_2\, U_2^{HS} \tag{71}$$

We write down now the evolution equations for the mean state of each population, defined as

$$\hat{U}_1^{HE} = \frac{U_1^{HE}}{n_1^{HE}}, \qquad \hat{U}_1^{A} = \frac{U_1^{A}}{n_1^{A}}, \qquad \hat{U}_2^{S} = \frac{U_2^{S}}{n_2^{S}}, \qquad \hat{U}_2^{HS} = \frac{U_2^{HS}}{n_2^{HS}}.$$

Combining the evolution equations for the number densities (57), (58), (63), (64) and those for the total internal states (67), (69), (70), (71), one has

$$\frac{\mathrm{d}\hat{U}_1^{HE}}{\mathrm{d}t} = \frac{1}{n_1^{HE}}\frac{\mathrm{d}U_1^{HE}}{\mathrm{d}t} - \frac{U_1^{HE}}{(n_1^{HE})^2}\frac{\mathrm{d}n_1^{HE}}{\mathrm{d}t} = \frac{\bar{\mu}_2^{(r)}\,\hat{I}_2}{n_1^{HE}}\left(n_2^S\,\hat{U}_2^S - n_2^{HS}\,\hat{U}_2^{HS} - n_2\,\hat{U}_1^{HE}\right) \tag{72}$$

$$\frac{\mathrm{d}\hat{U}_1^{A}}{\mathrm{d}t} = \frac{1}{n_1^{A}}\frac{\mathrm{d}U_1^{A}}{\mathrm{d}t} - \frac{U_1^{A}}{(n_1^{A})^2}\frac{\mathrm{d}n_1^{A}}{\mathrm{d}t} = 0 \tag{73}$$

$$\frac{\mathrm{d}\hat{U}_2^{S}}{\mathrm{d}t} = \frac{1}{n_2^{S}}\frac{\mathrm{d}U_2^{S}}{\mathrm{d}t} - \frac{U_2^{S}}{(n_2^{S})^2}\frac{\mathrm{d}n_2^{S}}{\mathrm{d}t} = -\frac{n_1^A}{n_2^S}\left(\bar{\eta}_{11}^{(r)}\,n_1^A + \bar{\mu}_1^{(r)}\,\hat{I}_1\right)\left(\hat{U}_1^A + \hat{U}_2^S\right) \tag{74}$$

$$\frac{\mathrm{d}\hat{U}_2^{HS}}{\mathrm{d}t} = \frac{1}{n_2^{HS}}\frac{\mathrm{d}U_2^{HS}}{\mathrm{d}t} - \frac{U_2^{HS}}{(n_2^{HS})^2}\frac{\mathrm{d}n_2^{HS}}{\mathrm{d}t} = -(1-\alpha)\,\bar{\eta}_{22}\,\frac{(n_2^S)^2}{n_2^{HS}}\left(\hat{U}_2^S + \hat{U}_2^{HS}\right) \tag{75}$$

5 Equilibrium States

5.1 Size of the Populations

Starting from the evolution equations for the size of the populations (Eqs. (57), (58), (63), (64)), the equilibrium states are solutions of the following system:

$$(1-2\beta)\,\overline{\eta}_{11}\,n_1^{HE}\,n_1^A + \overline{\eta}_{21}^{(r)}\,n_1^{HE}\,n_2 + \overline{\mu}_2^{(r)}\,\hat{I}_2\,n_2 = 0 \tag{76}$$

$$(2\beta-1)\,\overline{\eta}_{11}\,n_1^{HE}\,n_1^A - \overline{\eta}_{11}^{(r)}\,(n_1^A)^2 - \overline{\mu}_1^{(r)}\,\hat{I}_1\,n_1^A = 0 \tag{77}$$

$$-(1-\alpha)\,\overline{\eta}_{22}\,(n_2^S)^2 + \overline{\eta}_{11}^{(r)}\,(n_1^A)^2 - \overline{\eta}_{21}^{(r)}\,n_1^{HE}\,n_2^S - \overline{\mu}_2^{(r)}\,\hat{I}_2\,n_2^S + \overline{\mu}_1^{(r)}\,\hat{I}_1\,n_1^A = 0 \tag{78}$$

$$(1-\alpha)\,\overline{\eta}_{22}\,(n_2^S)^2 - \overline{\eta}_{21}^{(r)}\,n_1^{HE}\,n_2^{HS} - \overline{\mu}_2^{(r)}\,\hat{I}_2\,n_2^{HS} = 0 \tag{79}$$

These equations are not independent of each other; therefore, one can find an infinite family of equilibrium solutions.

(i) The above system admits a trivial solution corresponding to:

$$n_1^A = n_2^S = n_2^{HS} = 0 \tag{80}$$

while n_1^{HE} can take any positive value. Since the total number of individuals N given by (9) is constant, this equilibrium solution reads as $n_1^{HE} = N$. Therefore, it corresponds to the eradication of the pandemic.

(ii) The unique non-trivial solution of Eqs. (76)–(79), with $n_1^{HE} > 0$, $n_1^A > 0$, $n_2^S > 0$, $n_2^{HS} > 0$, is given by (endemic equilibrium):

$$n_1^A = (\overline{\eta}_{11}^{(r)})^{-1}[(2\beta - 1)\,\overline{\eta}_{11}\,n_1^{HE} - \overline{\mu}_1^{(r)}\,\hat{I}_1] \tag{81}$$

$$\begin{aligned} n_2^S = [2(1-\alpha)\overline{\eta}_{22}]^{-1}\Bigg\{ & -\overline{\eta}_{21}^{(r)}\,n_1^{HE} - \overline{\mu}_2^{(r)}\,\hat{I}_2 \\ & + \Bigg[\left(\overline{\eta}_{21}^{(r)2} + 4(1-\alpha)(2\beta-1)^2\,\frac{\overline{\eta}_{11}^2\,\overline{\eta}_{22}}{\overline{\eta}_{11}^{(r)}}\right)(n_1^{HE})^2 \\ & + \left(2\,\overline{\eta}_{21}^{(r)}\,\overline{\mu}_2^{(r)}\,\hat{I}_2 - 4(1-\alpha)\,(2\beta-1)\,\frac{\overline{\eta}_{11}\,\overline{\eta}_{22}}{\overline{\eta}_{11}^{(r)}}\,\overline{\mu}_1^{(r)}\,\hat{I}_1\right) n_1^{HE} + \overline{\mu}_2^{(r)2}\,\hat{I}_2^2\Bigg]^{\frac{1}{2}}\Bigg\} \end{aligned} \tag{82}$$

$$\begin{aligned} n_2^{HS} = & [\overline{\eta}_{11}^{(r)}\,(\overline{\mu}_2^{(r)}\,\hat{I}_2 + \overline{\eta}_{21}^{(r)}\,n_1^{HE})]^{-1}\,[(1-2\beta)^2\,\overline{\eta}_{11}^2\,(n_1^{HE})^2 \\ & -(2\beta-1)\,\overline{\eta}_{11}\,\overline{\mu}_1^{(r)}\,\hat{I}_1\,n_1^{HE}] - n_2^S \end{aligned} \tag{83}$$

In order to have $n_1^A > 0$, the following condition must be fulfilled:

$$n_1^{HE} > \frac{\overline{\mu}_1^{(r)}\,\hat{I}_1}{(2\beta-1)\,\overline{\eta}_{11}} \tag{84}$$

with $\beta > \frac{1}{2}$. Furthermore, n_2^S given by Eq. (82) is well defined if $\alpha \neq 1$.

We note that if

$$n_1^{HE} = \frac{\overline{\mu}_1^{(r)}\,\hat{I}_1}{(2\beta-1)\,\overline{\eta}_{11}}$$

then Eqs.(81)–(83) give $n_1^A = n_2^S = n_2^{HS} = 0$. Therefore, from Eq. (9) it follows $n_1^{HE} = N$. This means that condition (84) is equivalent to

$$N > \frac{\overline{\mu}_1^{(r)}\,\hat{I}_1}{(2\beta-1)\,\overline{\eta}_{11}}.$$

5.2 Mean State of the Populations

We analyze also the equilibrium solutions for the mean epidemiological state of each population. From Eq. (73), it follows:

$$\hat{U}_1^A = const. \tag{85}$$

Then, setting the left-hand side of Eqs. (72), (74), (75) equal to zero, and imposing that $n_1^{HE} > 0$, $n_1^A > 0$, $n_2^S > 0$, $n_2^{HS} > 0$, $\alpha \neq 1$, $\overline{\mu}_2^{(r)} \neq 0$, $\hat{I}_2 \neq 0$, we get

$$\hat{U}_2^{HS} = -\hat{U}_2^S \tag{86}$$

$$\hat{U}_1^A = -\hat{U}_2^S \tag{87}$$
$$\hat{U}_1^{HE} = \hat{U}_2^S \tag{88}$$

Rearranging the results given by Eqs. (86)–(88), one obtains:

$$\hat{U}_1^{HE} + \hat{U}_1^A = 0 \tag{89}$$
$$\hat{U}_2^S + \hat{U}_2^{HS} = 0 \tag{90}$$

Equations (85), (89), (90) allow us to infer that, when the equilibrium is reached, there is a perfect balance in terms of epidemiological state for the two groups of individuals within each population.

6 Stability of Equilibrium

In order to study the stability of the non-trivial equilibrium solutions for the population sizes, let us consider Eqs. (57)–(58) which form a closed system once we substitute n_2 with the following expression:

$$n_2 = N - n_1^{HE} - n_1^A \tag{91}$$

where N is the constant total number of individuals. Then, we can rewrite these equations in the form:

$$\begin{cases} \dfrac{\mathrm{d}n_1^{HE}}{\mathrm{d}t} = f(n_1^{HE}, n_1^A) \\ \dfrac{\mathrm{d}n_1^A}{\mathrm{d}t} = g(n_1^{HE}, n_1^A) \end{cases} \tag{92}$$

and apply the following

Theorem 6.1 *Let us suppose that* $(\tilde{n}_1^{HE}, \tilde{n}_1^A)$ *is an equilibrium point of the system* (92) *(under the hypothesis,* $f, g \in C^1$*) and that the Jacobian matrix:*

$$J = \begin{pmatrix} \dfrac{\partial f}{\partial n_1^{HE}} & \dfrac{\partial f}{\partial n_1^A} \\ \dfrac{\partial g}{\partial n_1^{HE}} & \dfrac{\partial g}{\partial n_1^A} \end{pmatrix}$$

evaluated at $(\tilde{n}_1^{HE}, \tilde{n}_1^A)$*, is not singular (that is,* $det(J) \neq 0$*), then:*

(i) *The equilibrium point* $(\tilde{n}_1^{HE}, \tilde{n}_1^A)$ *is (locally) asymptotically stable if all the eigenvalues of* J *have strictly negative real part;*
(ii) *The equilibrium point* $(\tilde{n}_1^{HE}, \tilde{n}_1^A)$ *is unstable if at least one eigenvalue of* J *has strictly positive real part.*

Remark 6.1 Theorem 6.1 holds in general for a system of m equations. Indeed, in our planar case $m = 2$, the stability conditions reported in Theorem 6.1 are equivalent to stating that an equilibrium point is (locally) asymptotically stable if and only if: $Tr(J) < 0$ and $det(J) > 0$, where $Tr(J)$ and $det(J)$ stand for 'trace' and 'determinant' of J, respectively.

Therefore, in order to analyze the stability of the equilibrium solution given in Sect. 5.1, we need to evaluate the sign of $Tr(J)$ and $det(J)$.

Taking into account that:

$$\frac{\partial f}{\partial n_1^{HE}}(\tilde{n}_1^{HE}, \tilde{n}_1^{A}) = (1-2\beta)\,\overline{\eta}_{11}\,\tilde{n}_1^{A} + \overline{\eta}_{21}^{(r)}\,(N - \tilde{n}_1^{HE} - \tilde{n}_1^{A}) - \overline{\eta}_{21}^{(r)}\,\tilde{n}_1^{HE} - \overline{\mu}_2^{(r)}\,\hat{I}_2 \tag{93}$$

$$\frac{\partial f}{\partial n_1^{A}}(\tilde{n}_1^{HE}, \tilde{n}_1^{A}) = (1-2\beta)\,\overline{\eta}_{11}\,\tilde{n}_1^{HE} - \overline{\eta}_{21}^{(r)}\,\tilde{n}_1^{HE} - \overline{\mu}_2^{(r)}\,\hat{I}_2 \tag{94}$$

$$\frac{\partial g}{\partial n_1^{HE}}(\tilde{n}_1^{HE}, \tilde{n}_1^{A}) = (2\beta-1)\,\overline{\eta}_{11}\,\tilde{n}_1^{A} \tag{95}$$

$$\frac{\partial g}{\partial n_1^{A}}(\tilde{n}_1^{HE}, \tilde{n}_1^{A}) = (2\beta-1)\,\overline{\eta}_{11}\,\tilde{n}_1^{HE} - 2\,\overline{\eta}_{11}^{(r)}\,\tilde{n}_1^{A} - \overline{\mu}_1^{(r)}\,\hat{I}_1 \tag{96}$$

we get

$$\begin{aligned} Tr(J) &= \frac{\partial f}{\partial n_1^{HE}}(\tilde{n}_1^{HE}, \tilde{n}_1^{A}) + \frac{\partial g}{\partial n_1^{A}}(\tilde{n}_1^{HE}, \tilde{n}_1^{A}) \\ &= -(2\beta-1)\frac{\overline{\eta}_{11}}{\overline{\eta}_{11}^{(r)}}\left[(2\beta-1)\,\overline{\eta}_{11}\,\tilde{n}_1^{HE} - \overline{\mu}_1^{(r)}\,\hat{I}_1\right] \\ &\quad + \frac{(2\beta-1)\,\overline{\eta}_{21}^{(r)}\,\overline{\eta}_{11}\,\tilde{n}_1^{HE}}{\overline{\eta}_{11}^{(r)}(\overline{\eta}_{21}^{(r)}\,\tilde{n}_1^{HE} + \overline{\mu}_2^{(r)}\,\hat{I}_2)} \\ &\quad \left[(2\beta-1)\,\overline{\eta}_{11}\,\tilde{n}_1^{HE} - \overline{\mu}_1^{(r)}\,\hat{I}_1\right] - \overline{\eta}_{21}^{(r)}\,\tilde{n}_1^{HE} - \overline{\mu}_2^{(r)}\,\hat{I}_2 \\ &\quad - \left[(2\beta-1)\,\overline{\eta}_{11}\,\tilde{n}_1^{HE} - \overline{\mu}_1^{(r)}\,\hat{I}_1\right] \end{aligned} \tag{97}$$

Since in Eq. (97) the terms in the square brackets must be positive in equilibrium conditions and $\beta > \frac{1}{2}$, then $Tr(J) < 0$ if the following inequality holds:

$$\begin{aligned} &(2\beta-1)\,\overline{\eta}_{11}\,\overline{\mu}_2^{(r)}\,\hat{I}_2\,x + (2\beta-1)\,\overline{\eta}_{11}\,\overline{\eta}_{21}^{(r)}\,\tilde{n}_1^{HE}\,x \\ &+\overline{\eta}_{11}^{(r)}\left(\overline{\eta}_{21}^{(r)}\,\tilde{n}_1^{HE} + \overline{\mu}_2^{(r)}\,\hat{I}_2\right)x + \overline{\eta}_{11}^{(r)}\left(\overline{\eta}_{21}^{(r)}\,\tilde{n}_1^{HE} + \overline{\mu}_2^{(r)}\,\hat{I}_2\right)^2 \\ &> (2\beta-1)\,\overline{\eta}_{21}^{(r)}\,\overline{\eta}_{11}\,\tilde{n}_1^{HE}\,x \end{aligned} \tag{98}$$

where

$$x = (2\beta - 1)\,\overline{\eta}_{11}\,\tilde{n}_1^{HE} - \overline{\mu}_1^{(r)}\,\hat{I}_1 > 0. \tag{99}$$

By observing that all the terms on the left-hand side are positive and that the second term is equal to the one on the right-hand side, we can conclude that the inequality (98) is always verified.

Analogously, we can compute:

$$\begin{aligned}
\det(J) &= \frac{\partial f}{\partial n_1^{HE}}(\tilde{n}_1^{HE}, \tilde{n}_1^{A})\,\frac{\partial g}{\partial n_1^{A}}(\tilde{n}_1^{HE}, \tilde{n}_1^{A}) - \frac{\partial f}{\partial n_1^{A}}(\tilde{n}_1^{HE}, \tilde{n}_1^{A})\,\frac{\partial g}{\partial n_1^{HE}}(\tilde{n}_1^{HE}, \tilde{n}_1^{A}) \\
&= \left\{ -(2\beta - 1)\,\overline{\eta}_{11}\,\tilde{n}_1^{A} + \overline{\eta}_{21}^{(r)}\,(N - \tilde{n}_1^{HE} - \tilde{n}_1^{A}) - [\overline{\eta}_{21}^{(r)}\,\tilde{n}_1^{HE} + \overline{\mu}_2^{(r)}\,\hat{I}_2] \right\} \\
&\quad \cdot \left\{ [(2\beta - 1)\,\overline{\eta}_{11}\,\tilde{n}_1^{HE} - \overline{\mu}_1^{(r)}\,\hat{I}_1] - 2\,\overline{\eta}_{11}^{(r)}\,\tilde{n}_1^{A} \right\} \\
&\quad + \left\{ (2\beta - 1)\,\overline{\eta}_{11}\,\tilde{n}_1^{HE} + [\overline{\eta}_{21}^{(r)}\,\tilde{n}_1^{HE} + \overline{\mu}_2^{(r)}\,\hat{I}_2] \right\} (2\beta - 1)\,\overline{\eta}_{11}\,\tilde{n}_1^{A} \\
&= T_1 + T_2
\end{aligned} \tag{100}$$

where

$$\begin{aligned}
T_1 &= \left\{ -(2\beta - 1)\,\overline{\eta}_{11}\,\tilde{n}_1^{A} + \overline{\eta}_{21}^{(r)}\,(N - \tilde{n}_1^{HE} - \tilde{n}_1^{A}) - [\overline{\eta}_{21}^{(r)}\,\tilde{n}_1^{HE} + \overline{\mu}_2^{(r)}\,\hat{I}_2] \right\} \\
&\quad \cdot \left\{ [(2\beta - 1)\,\overline{\eta}_{11}\,\tilde{n}_1^{HE} - \overline{\mu}_1^{(r)}\,\hat{I}_1] - 2\,\overline{\eta}_{11}^{(r)}\,\tilde{n}_1^{A} \right\}
\end{aligned} \tag{101}$$

$$T_2 = \left\{ (2\beta - 1)\,\overline{\eta}_{11}\,\tilde{n}_1^{HE} + [\overline{\eta}_{21}^{(r)}\,\tilde{n}_1^{HE} + \overline{\mu}_2^{(r)}\,\hat{I}_2] \right\} (2\beta - 1)\,\overline{\eta}_{11}\,\tilde{n}_1^{A} \tag{102}$$

Since $T_2 > 0$, in order to prove that $det(J) > 0$, we have to only evaluate the sign of T_1:

$$T_1 = (2\beta - 1)\,\frac{\overline{\eta}_{11}}{\overline{\eta}_{11}^{(r)}}\,x^2 - \frac{(2\beta - 1)\,\overline{\eta}_{21}^{(r)}\,\overline{\eta}_{11}\,\tilde{n}_1^{HE}}{\overline{\eta}_{11}^{(r)}(\overline{\eta}_{21}^{(r)}\,\tilde{n}_1^{HE} + \overline{\mu}_2^{(r)}\,\hat{I}_2)}x^2 + (\overline{\eta}_{21}^{(r)}\,\tilde{n}_1^{HE} + \overline{\mu}_2^{(r)}\,\hat{I}_2)\,x \tag{103}$$

where x is a positive quantity given by (99). From (103), we deduce that $T_1 > 0$ if

$$\begin{aligned}
&(2\beta - 1)\,\overline{\eta}_{11}\,\overline{\mu}_2^{(r)}\,\hat{I}_2\,x + (2\beta - 1)\,\overline{\eta}_{11}\,\overline{\eta}_{21}^{(r)}\,\tilde{n}_1^{HE}\,x + \overline{\eta}_{11}^{(r)}\left(\overline{\eta}_{21}^{(r)}\,\tilde{n}_1^{HE} + \overline{\mu}_2^{(r)}\,\hat{I}_2\right)^2 \\
&\qquad > (2\beta - 1)\,\overline{\eta}_{11}\,\overline{\eta}_{21}^{(r)}\,\tilde{n}_1^{HE}\,x
\end{aligned} \tag{104}$$

Since all the terms on the left-hand side are positive and the second term is equal to the one on the right-hand side, we infer that the inequality (104) is always verified.

On the other hand, evaluating the expressions (93)–(96) in correspondence of the trivial equilibrium solution $(n_1^{HE}, n_1^A) = (N, 0)$, we easily get that both eigenvalues of the Jacobian matrix are negative (the equilibrium is stable) if and only if

$$N < \frac{\overline{\mu}_1^{(r)}\, \hat{I}_1}{(2\beta - 1)\, \overline{\eta}_{11}}$$

that is, when the endemic equilibrium does not exist.

7 Numerical Simulations

In the following, we present some numerical test cases in order to assess the ability of our contact-based model to qualitatively reproduce the main features of recent SARS-CoV-2 spread. We have numerically integrated Eqs. (57) and (58) until an equilibrium solution has been obtained. By taking into account that the total number of individuals N is conserved, we have substituted

$$n_2 = N - n_1^{HE} - n_1^A \tag{105}$$

in Eq. (57). Thus, Eqs. (57) and (58) form a closed system of equations that can be solved to give the temporal evolution of the number densities of healthy individuals (n_1^{HE}) and of asymptomatic carriers (n_1^A). In all the numerical simulations presented below we have fixed $N = 1$. To estimate the numerical error, we have compared the equilibrium solution obtained by integrating Eqs. (57) and (58) and the one computed analytically using the formulas reported in Sect. 5.1 (where the terms have been rearranged in order to insert in Eq. (83) the expression (105) with $N = 1$). The agreement has proved to be very good in all cases considered with the error always within 0.1%.

We remark that our numerical simulations aim only at providing a qualitative description of the macroscopic evolution of the pandemic corresponding to our model, and plots do not refer to real data. We will see in the figures that our model is able to predict the subsequent waves of a pandemic recently observed in SARS-CoV-2 evolution, and analogous scenarios might occur also in other contact-based infections.

Test case (1).

Here we investigate the impact of an extremely contagious variant by setting $\beta = 1$ in the stochastic law modeling the interactions between a healthy individual and an asymptomatic carrier (formula (29)).

(1.a) First, we consider a situation where social restrictions are not applied. Therefore, we assume that interactions between individuals without symptoms (described by the parameter $\bar{\eta}_{11}$) are much more probable than others:

$$\bar{\eta}_{11} = 1, \qquad \bar{\eta}_{11}^{(r)} = 0.1, \qquad \bar{\eta}_{21}^{(r)} = 0.1.$$

Furthermore, we take into account the action of the immune system by choosing:

$$\bar{\mu}_1^{(r)}\,\hat{I}_1 = 0.3, \qquad \bar{\mu}_2^{(r)}\,\hat{I}_2 = 0.05.$$

Starting from the initial conditions

$$(n_1^{HE}, n_1^A, n_2)(t=0) = (0.8, 0.1, 0.1) \tag{106}$$

Equations (57) and (58) have been integrated and the time evolution of the number density of healthy individuals (n_1^{HE}), positive asymptomatic (n_1^A) and ill people (n_2) is reported in Fig. 1a. In the same picture, the profile of the time-dependent effective reproduction number R_0 (Eq. 65) is also shown in order to quantify the effectiveness of virus containment strategies. Since for the chosen parameters the condition (84) is fulfilled, our system of equations (57) and (58) admits a non-trivial equilibrium solution given by

$$(n_1^{HE}, n_1^A, n_2) = (0.3141, 0.1411, 0.5448). \tag{107}$$

In the framework of an epidemiological analysis, it is of paramount importance to also evaluate how an endemic equilibrium is achieved. Therefore, in Fig. 2a the phase portrait, corresponding to the system (57)–(58), is shown in the three-dimensional space (n_1^{HE}, n_1^A, n_2). From this picture, a characteristic spiral shape of the curves is evident with peaks and troughs of infections. This behavior closely resembles the concept of an epidemic wave. Indeed, the SARS-CoV-2 pandemic developed as a series of waves: surges of new infections followed by declines. Although there is no a common idea among researchers of what constitutes an epidemic wave, a useful working definition has been proposed in Zhang et al. (2021), where this concept has been linked to the profile of the effective reproduction number R_0. If R_0 is larger than 1 for a sustained period, one can identify this time as an upward period for the epidemic wave. On the contrary, if R_0 is smaller than 1 for a sustained period, this time can be identified as a downward period for the epidemic wave. Relying on this definition, one can infer from Fig. 1a the existence of two pandemic waves as suggested also by the phase portrait in Fig. 2a.

(1.b) In the following, with respect to the test case (1.a), we consider an epidemic scenario in which treatments against the disease are more effective. Therefore, leaving all other parameters unchanged, we increase the value of $\bar{\eta}_{21}^{(r)}$ (which describes the rate of interaction between the medical staff and the infected individuals with symptoms) by setting $\bar{\eta}_{21}^{(r)} = 0.4$. Indeed, in the context of our model, a large value of this parameter indicates a high transition rate from population 2 to population 1 (healthy individuals). Again, starting from the initial conditions

$$(n_1^{HE}, n_1^A, n_2)(t=0) = (0.8, 0.1, 0.1),$$

Equations (57) and (58) have been integrated and the time evolution of the number densities n_1^{HE}, n_1^A, n_2 is plotted in Fig. 1b along with the profile of the time-dependent

effective reproduction number R_0. For this test case, the non-trivial equilibrium solution is given by

$$(n_1^{HE}, n_1^A, n_2) = (0.3241, 0.2412, 0.4347). \tag{108}$$

As expected, the number of sick people is lower than in the previous case (1.a) (see expression (107)). To complete the scenario, the phase portrait is shown in Fig. 2b. From these pictures, we note that the duration of the pandemic is shorter and that the peak of R_0 is lower than in the test case (1.a), while the phase portraits are quite similar.

(1.c) In this test, we assess the impact of vaccination, which affects the response of both the innate and adaptive immune system. In particular, with respect to the test case (1.a), we increase the term $(\bar{\mu}_2^{(r)}\,\hat{I}_2)$ (which describes the overall response of the adaptive immune system on individuals belonging to population 2) and we decrease the term $(\bar{\mu}_1^{(r)}\,\hat{I}_1)$ (which models the average action of the innate immune system on asymptomatic individuals) by setting

$$\bar{\mu}_1^{(r)}\,\hat{I}_1 = 0.1, \qquad \bar{\mu}_2^{(r)}\,\hat{I}_2 = 0.2.$$

In the framework of the model we derived, large values of the term $(\bar{\mu}_2^{(r)}\,\hat{I}_2)$ indicate that a significant fraction of sick people recovers without specific treatments, while small values of the term $(\bar{\mu}_1^{(r)}\,\hat{I}_1)$ denote a negligible probability for the hyperinflammation phenomenon to occur. Starting from the same initial conditions previously considered in the tests (1.a) and (1.b),

$$(n_1^{HE}, n_1^A, n_2)(t = 0) = (0.8, 0.1, 0.1),$$

Equations (57) and (58) have been integrated and the time evolution of the number densities n_1^{HE}, n_1^A, n_2 along with the trend of the effective reproduction number R_0 is shown in Fig. 1c. For the set of parameters considered, our system of equations admits a non-trivial equilibrium solution given by

$$(n_1^{HE}, n_1^A, n_2) = (0.1501, 0.5010, 0.3489). \tag{109}$$

Compared to previous tests, the number of ill persons belonging to population 2 is significantly reduced. The large fraction of carriers can be explained by taking into account that we are analyzing an extremely contagious variant ($\beta = 1$) in which each healthy individual interacting with a positive asymptomatic becomes infectious. Therefore, due to the large number of healthy people, also the number of positive asymptomatic persons will be higher than in previous tests. Furthermore, this trend is perfectly in line with the realistic situation created by the administration of Covid-19 vaccines, which have reduced the number of ill individuals without, however, preventing people from contracting the virus. Figure 1c shows that the convergence to equilibrium is faster than in previous tests without subsequent epidemic waves, as confirmed by the phase portrait given in Fig. 2c.

Test case (2).

In the following, we analyze the evolution of an epidemic driven by a variant with a lower transmission rate than in the *test case (1)*. Therefore, we set $\beta = 0.7$.

(2.a) Here the parameters we use to integrate Eqs. (57) and (58) along with the initial conditions are the same as in test (1.a). In this case, the non-trivial equilibrium solution is given by

$$(n_1^{HE}, n_1^A, n_2) = (0.7671, 0.0684, 0.1646). \tag{110}$$

As expected, the number of healthy individuals is much higher than in test (1.a), and consequently, the number of sick people is much lower. Looking at the time evolution of the number densities n_1^{HE}, n_1^A, n_2 and of the effective reproduction number R_0 shown in Fig. 3a, one infers that there are no epidemic waves and the outbreak dies out very quickly. These features are also confirmed by the phase portrait reported in Fig. 4a.

(2.b) For this simulation, we have chosen the same values of the parameters and of the initial conditions as in test (1.b) in order to integrate Eqs. (57) and (58). The non-trivial equilibrium solution obtained is

$$(n_1^{HE}, n_1^A, n_2) = (0.7795, 0.1182, 0.1023). \tag{111}$$

From the comparison with the previous case (2.a), it can be deduced that, as regards variants with low transmission rates, the effectiveness of medical treatments is not a decisive factor in reducing the number of sick people, since the equilibrium values differ only slightly. Indeed, the time evolution of the number densities n_1^{HE}, n_1^A, n_2 and of the effective reproduction number R_0, shown in Fig. 3b, along with the phase portrait, presented in Fig. 4b, indicates that the duration of the epidemic is shorter than in the case (2.a).

(2.c) In order to evaluate the effects of vaccination, we choose the same parameters considered in test *(1.c)*. Starting from the same initial conditions, the integration of Eqs. (57) and (58) leads to the following endemic equilibrium solution

$$(n_1^{HE}, n_1^A, n_2) = (0.3516, 0.4063, 0.2422). \tag{112}$$

The comparison of result (112) with formulas (110) and (111) allows one to conclude that, for variants with low transmission rates, vaccination is not so effective, in terms of reducing the number of sick people, as it has been observed in the case of highly contagious variants (see test *(1.c)*). However, the time evolution of the number densities n_1^{HE}, n_1^A, n_2 and of the effective reproduction number R_0, shown in Fig. 3c, along with the phase portrait, reported in Fig. 4c, confirms that the epidemic ends very quickly, as expected.

Beyond the simulations presented above, we have further checked numerically that, if we introduce lockdown measures decreasing the value of the parameter $\bar{\eta}_{11}$ in the test cases (1.a) and (2.a), that is the rate of interaction between individuals without symptoms, then the number of sick persons is drastically reduced. As a final remark, it is interesting to note how the peaks in the temporal evolution of the effective reproduction

number R_0 are always in correspondence (even if not exactly coinciding) with the peaks in the number density profile of positive asymptomatic individuals (n_1^A), while the maximum value of the number density of sick people (n_2) is slightly postponed in time. This trend reflects what has been observed in the Covid-19 pandemic, where the peak of the infection has always been followed (during different waves), with a slight time delay, by the peak in the number of ill persons.

It would be also interesting to simulate the kinetic system (14) and (19), possibly adapting numerical methods for kinetic equations proposed in Bertaglia and Pareschi (2021), Boscheri et al. (2021) and Degond et al. (2004), and this is scheduled as future work.

8 Concluding Remarks

In this work, we have exploited the statistical mechanics methods in order to model the human-to-human mechanisms of a contact-based infection and in particular of SARS-CoV-2 transmission. Starting from a description of the interactions between individuals based on the Boltzmann equation, we have derived a set of evolution equations for the size and mean state of each considered population, that is, healthy people, positive asymptomatic, positive symptomatic, and hospitalized persons. Unlike the epidemiological models that have been developed within the kinetic theory framework in the last few years, our approach does not rely on one of the existing compartmental models, but we derive a new system of macroscopic evolution equations, which in particular aims to account for the characteristics of Covid-19. Indeed, our model focuses on the role of positive asymptomatic individuals in triggering the spread of SARS-CoV-2 virus. Asymptomatic transmission has been considered as the "Achilles' heel" of Covid-19 control strategies. Actually, several studies have demonstrated that asymptomatic carriers have infected a similar number of people as symptomatic individuals (Boyton and Altmann 2021; Wilmes et al. 2021). Beyond a trivial equilibrium solution corresponding to $n_1^A = n_2^S = n_2^{HS} = 0$ (that is, the eradication of the disease), our model predicts, under suitable conditions on infection parameters, the existence of an endemic equilibrium which is always asymptotically stable.

It is worth to highlight that, in the present paper, the study of the spread of an infectious disease is carried out starting from a system of evolution equations for the distribution functions of interacting populations, while classical compartmental models are formulated in terms of densities, that is, the average number of individuals assigned to different categories (susceptible, infected and recovered, in the case of the SIR model). This approach allows us to take into account the details of the interaction between people with different viral loads. In the framework of the Boltzmann equation, the same binary interaction mechanism responsible for the spread of contagion is exploited to model the recovery of an infected person thanks to the treatments of the medical staff. These interactions are described by the quadratic Boltzmann operator. Only the action of the immune system gives rise to a linear collision operator. Compared to our formulation, the compartmental models assume a similar mechanism for the disease transmission through a direct contact between a susceptible person and an infected one, leading to a quadratic term in the evolution equations. But the recov-

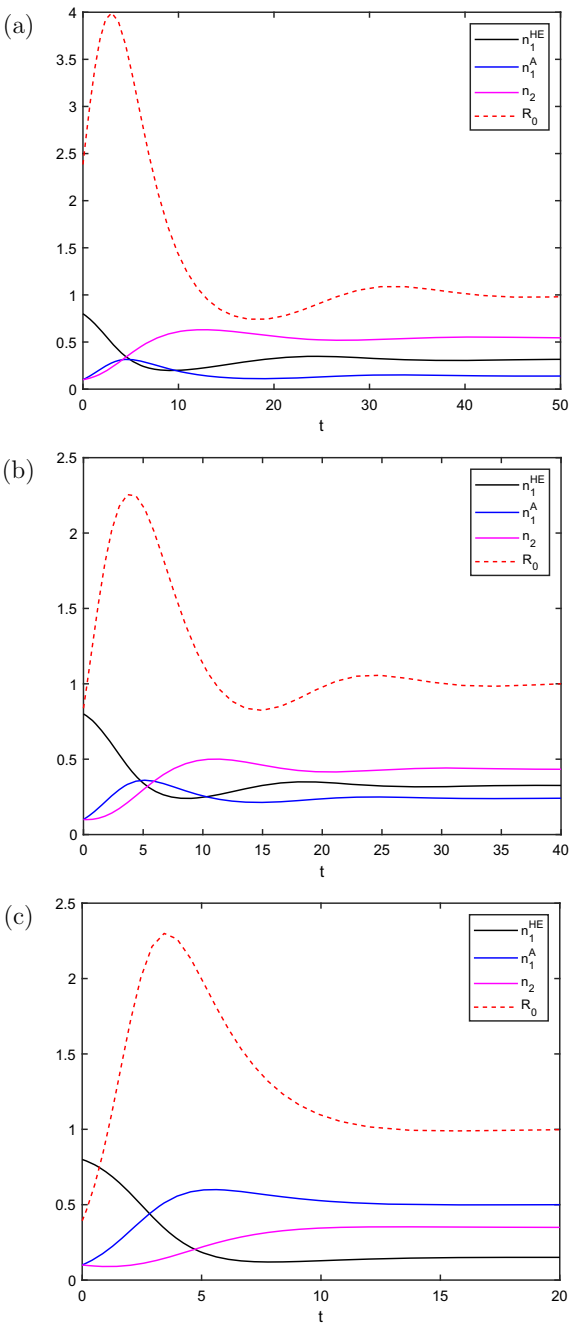

Fig. 1 Time evolution of the initial data $(n_1^{HE}, n_1^A, n_2)(t = 0) = (0.8, 0.1, 0.1)$ and of the reproduction number R_0 with $\beta = 1$, $\bar{\eta}_{11} = 1$, $\bar{\eta}_{11}^{(r)} = 0.1$. Panel **a**: $\bar{\eta}_{21}^{(r)} = 0.1$, $\bar{\mu}_1^{(r)}\,\hat{I}_1 = 0.3$, $\bar{\mu}_2^{(r)}\,\hat{I}_2 = 0.05$. Panel **b**: $\bar{\eta}_{21}^{(r)} = 0.4$, $\bar{\mu}_1^{(r)}\,\hat{I}_1 = 0.3$, $\bar{\mu}_2^{(r)}\,\hat{I}_2 = 0.05$. Panel **c**: $\bar{\eta}_{21}^{(r)} = 0.1$, $\bar{\mu}_1^{(r)}\,\hat{I}_1 = 0.1$, $\bar{\mu}_2^{(r)}\,\hat{I}_2 = 0.2$

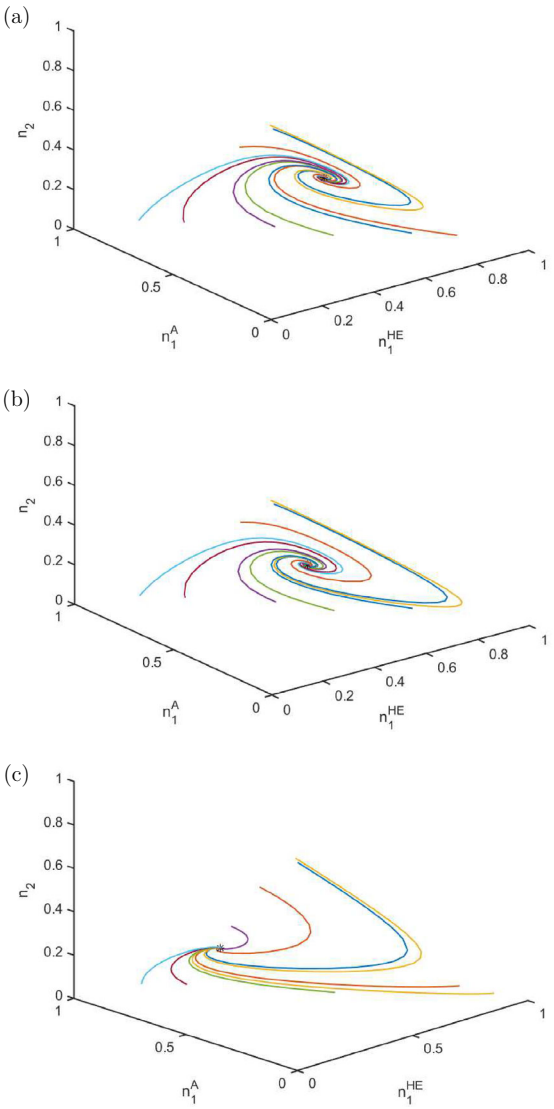

Fig. 2 Phase portrait of the evolution of n_1^{HE}, n_1^A, n_2 for a variant with contagion rate $\beta = 1$, and $\bar{\eta}_{11} = 1$, $\bar{\eta}_{11}^{(r)} = 0.1$. Panel **a**: $\bar{\eta}_{21}^{(r)} = 0.1$, $\bar{\mu}_1^{(r)} \hat{I}_1 = 0.3$, $\bar{\mu}_2^{(r)} \hat{I}_2 = 0.05$. Panel **b**: $\bar{\eta}_{21}^{(r)} = 0.4$, $\bar{\mu}_1^{(r)} \hat{I}_1 = 0.3$, $\bar{\mu}_2^{(r)} \hat{I}_2 = 0.05$. Panel **c**: $\bar{\eta}_{21}^{(r)} = 0.1$, $\bar{\mu}_1^{(r)} \hat{I}_1 = 0.1$, $\bar{\mu}_2^{(r)} \hat{I}_2 = 0.2$

ery of individuals is always supposed to occur at a rate proportional to the number of infectives, thus giving only a linear contribution to the model. Based on these remarks, in the following, we will show that the macroscopic equations for the evolution of the size of the populations considered in this work reduce to the classical SIS model, under suitable assumptions. In the SIS model, the population is divided only in two groups: the susceptible (S) and the infected (I) (Hethcote 2000). It is called SIS model since individuals return to the susceptible class when they recover from the infection. Let us identify in our study the healthy people (n_1^{HE}) with the susceptibles, and the positive

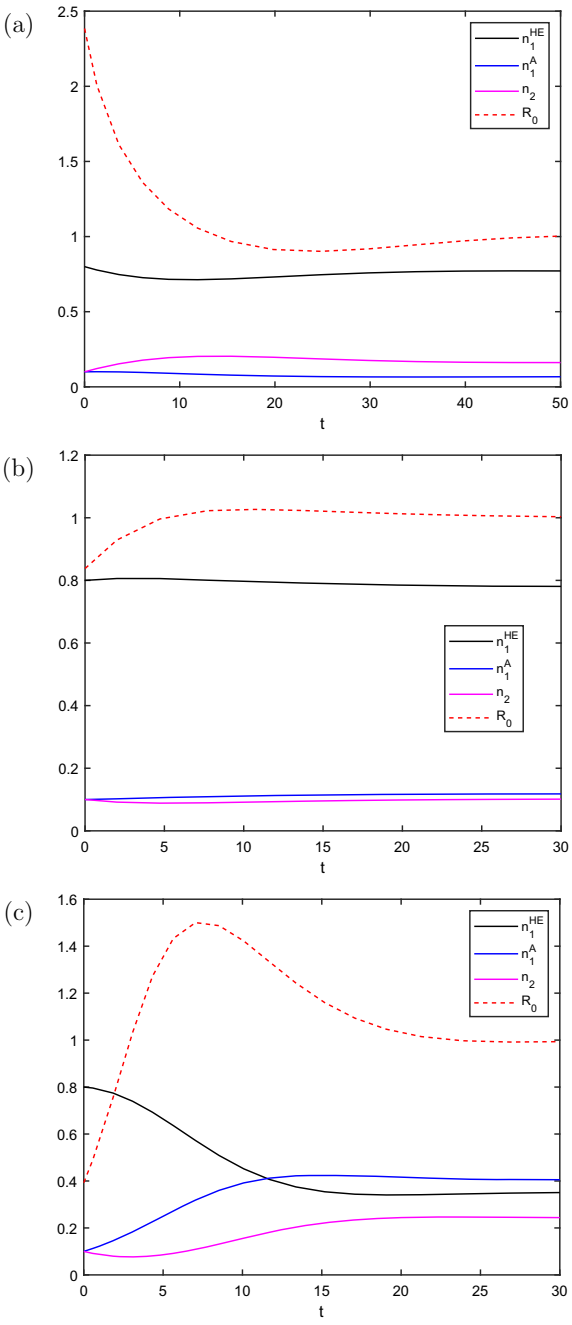

Fig. 3 Time evolution of the initial data $(n_1^{HE}, n_1^A, n_2)(t = 0) = (0.8, 0.1, 0.1)$ and of the reproduction number R_0 with $\beta = 0.7$, $\bar{\eta}_{11} = 1$, $\bar{\eta}_{11}^{(r)} = 0.1$. Panel **a**: $\bar{\eta}_{21}^{(r)} = 0.1$, $\bar{\mu}_1^{(r)}\,\hat{I}_1 = 0.3$, $\bar{\mu}_2^{(r)}\,\hat{I}_2 = 0.05$. Panel **b**: $\bar{\eta}_{21}^{(r)} = 0.4$, $\bar{\mu}_1^{(r)}\,\hat{I}_1 = 0.3$, $\bar{\mu}_2^{(r)}\,\hat{I}_2 = 0.05$. Panel **c**: $\bar{\eta}_{21}^{(r)} = 0.1$, $\bar{\mu}_1^{(r)}\,\hat{I}_1 = 0.1$, $\bar{\mu}_2^{(r)}\,\hat{I}_2 = 0.2$

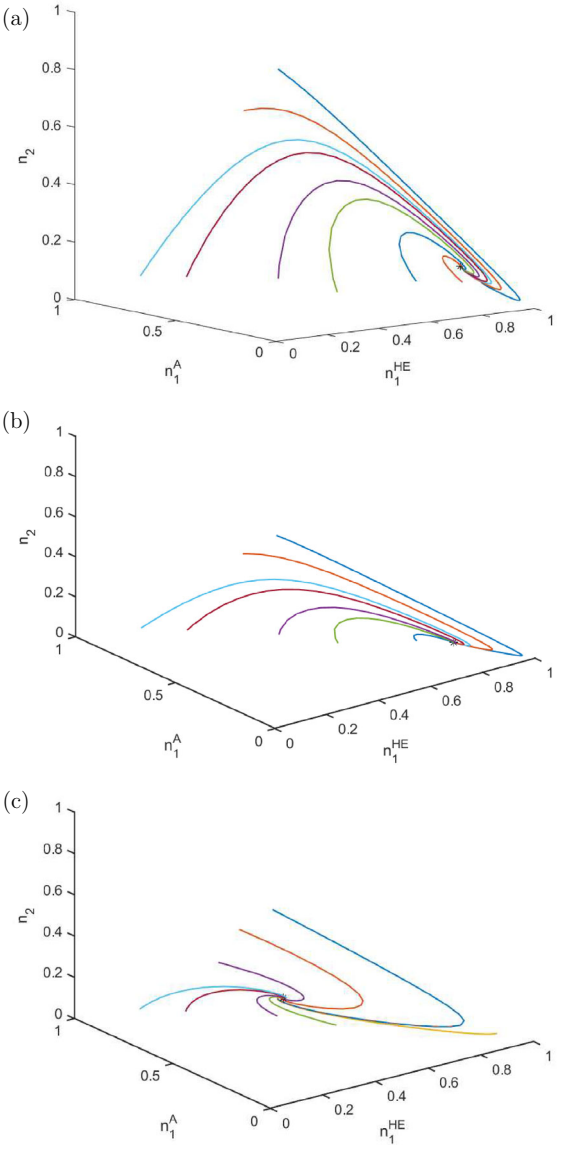

Fig. 4 Phase portrait of the evolution of n_1^{HE}, n_1^A, n_2 for a variant with contagion rate $\beta = 0.7$, and $\bar{\eta}_{11} = 1$, $\bar{\eta}_{11}^{(r)} = 0.1$. Panel **a**: $\bar{\eta}_{21}^{(r)} = 0.1$, $\bar{\mu}_1^{(r)} \hat{I}_1 = 0.3$, $\bar{\mu}_2^{(r)} \hat{I}_2 = 0.05$. Panel **b**: $\bar{\eta}_{21}^{(r)} = 0.4$, $\bar{\mu}_1^{(r)} \hat{I}_1 = 0.3$, $\bar{\mu}_2^{(r)} \hat{I}_2 = 0.05$. Panel **c**: $\bar{\eta}_{21}^{(r)} = 0.1$, $\bar{\mu}_1^{(r)} \hat{I}_1 = 0.1$, $\bar{\mu}_2^{(r)} \hat{I}_2 = 0.2$

asymptomatic (n_1^A), the positive symptomatic (n_2^S), and the hospitalized persons (n_2^{HS}) with the infective class, as follows:

$$\begin{cases} n_1^{HE} = S \\ n_1^A + n_2 = I \end{cases} \tag{113}$$

Adding equations (53) and (58), one gets

$$\frac{\mathrm{d}I}{\mathrm{d}t} = (2\beta - 1)\,\overline{\eta}_{11}\,S\,n_1^A - \overline{\eta}_{21}^{(r)}\,S\,n_2 - \overline{\mu}_2^{(r)}\,\hat{I}_2\,n_2. \tag{114}$$

Since in the SIS model the recovery of infected individuals gives a linear contribution, we have to require that the second term on the right-hand side of Eq. (114) (which is quadratic) vanishes, by putting $\overline{\eta}_{21}^{(r)} = 0$. In our analysis, this is equivalent to assuming that there are no effective treatments for the disease and that the recovery can only occur thanks to the action of the immune system. Thus, Eq. (114) with this additional assumption reads:

$$\frac{\mathrm{d}I}{\mathrm{d}t} = (2\beta - 1)\,\overline{\eta}_{11}\,S\,n_1^A - \overline{\mu}_2^{(r)}\,\hat{I}_2\,n_2. \tag{115}$$

Since in the SIS model there is no distinction between infected people with or without symptoms, the densities n_1^A and n_2 can be replaced with the generic infective class I. Indeed, in our study $\overline{\eta}_{11}$ is the rate of interaction between individuals of population 1, thus $\overline{\eta}_{11}\,n_2 = 0$, and we can substitute I, given by the second equation of (113), for n_1^A in the first term on the right-hand side of Eq. (115). In a similar way, since the adaptive immune system acts only on infected people with symptoms, then $\overline{\mu}_2^{(r)}\,n_1^A = 0$, and we can replace n_2 with I in the second term on the right-hand side of Eq. (115). Therefore, Eq. (115) becomes

$$\frac{\mathrm{d}I}{\mathrm{d}t} = [(2\beta - 1)\,\overline{\eta}_{11}]\,S\,I - [\overline{\mu}_2^{(r)}\,\hat{I}_2]\,I. \tag{116}$$

Taking advantage of the same assumptions considered above, Eq. (57) can be rewritten as follows:

$$\frac{\mathrm{d}S}{\mathrm{d}t} = -[(2\beta - 1)\,\overline{\eta}_{11}]\,S\,I + [\overline{\mu}_2^{(r)}\,\hat{I}_2]\,I. \tag{117}$$

Equations (116) and (117) have the formal structure of the SIS model.

This comparison is not reductive, since, even taking into account more sophisticated extensions of classical compartmental models, the methodology for reducing our system of equations to them is the same as illustrated above. As an example, let us mention the SIDARTHE model recently proposed to describe the COVID-19 epidemic (Giordano et al. 2020). This dynamical system considers eight stages of disease, discriminating between detected and undetected cases of infection and on the severity of their symptoms. But, despite the greater complexity compared to classical compartmental models, the mathematical structure is the same: a system of differential equations where the spread of contagion, due to contacts between an infectious and a susceptible person, gives rise to quadratic terms, while the recovery and the transition to classes of individuals with a higher level of infection are modeled as linear contributions. These characteristics make the SIDARTHE system intrinsically different

from our model where the dynamics of the epidemic can be traced back to the binary interaction between individuals (except the immune response).

Beyond a rigorous mathematical identification, our model is able to reproduce some aspects of qualitative dynamics of infectious diseases predicted by classical compartmental models. In particular, we have proved the existence of an endemic equilibrium which is also typical of compartmental models allowing for re-infections (like the SIS model) or models with vital dynamics (which include births and deaths). Indeed, in a SIR model with vital dynamics it occurs that, after the fraction of infected has been reduced below a certain threshold, the number of susceptible individuals slowly starts to increase due to the births of new susceptibles. When the susceptible fraction gets large enough, a second smaller epidemic arises and so on, as the path spirals toward the endemic equilibrium point. The existence of epidemic waves, that is, surges of new infections followed by declines, has been also predicted by our model. Actually, Figs. 2 and 4 show that the approach to endemic equilibrium is described by spiral-shaped curves.

To be more specific, we highlight below how different aspects of an infectious disease transmission can be addressed by changing the value of some relevant parameters of our model, with a particular focus on the SARS-CoV-2 spread.

(i) The impact of the contagiousness of new variants. By setting $\beta = 1$, in the stochastic law modeling the interactions between a healthy individual and a positive asymptomatic, an extremely contagious disease is described, while lower values of β account for less infectious scenarios.

(ii) The effects of government restrictions aimed at limiting the mobility of individuals. In particular, assuming a high rate of interaction between individuals without symptoms (e.g., $\overline{\eta}_{11} = 1$) means that such limitations are not applied, while lower values of $\overline{\eta}_{11}$ describe lockdown situations.

(iii) The effectiveness of specific medical treatments. The key parameter in this respect is $\overline{\eta}_{21}^{(r)}$, which describes the rate of interaction between the medical staff and the infected people belonging to population 2. If one takes increasing values of $\overline{\eta}_{21}^{(r)}$, our model equations allow to study the efficacy of new drugs in order to control the spread of the disease until its complete (possibly) eradication.

(iv) The role of the innate and adaptive immunity in setting the severity of Covid-19. The peculiarity of SARS-CoV-2 infection is traced back to a complex interplay between the virus and the immune system. It involves pathogenic cell activation leading to hyperinflammation with a major complication of the disease. This aspect can be taken into account in the macroscopic equations we derived by choosing large values of the term $(\overline{\mu}_1^{(r)}\, \hat{I}_1)$, which models the average action of the innate immune system on asymptomatic individuals (who have already contracted the virus). Furthermore, relying on clinical data, our model provides for the possibility that ill persons recover without specific treatments, by assuming large values of the term $(\overline{\mu}_2^{(r)}\, \hat{I}_2)$, which describes the overall response of the adaptive immune system on individuals belonging to population 2. Since adaptive immunity can be acquired through the administration of vaccines, which in turn increase the anti-viral activity of some innate immune cells, our system of

equations allows one also to assess the impact of vaccination by increasing the term $(\overline{\mu}_2^{(r)}\,\hat{I}_2)$ and, at the same time, decreasing $(\overline{\mu}_1^{(r)}\,\hat{I}_1)$.

The numerical test cases presented in Sect. 7 highlight the ability of our model to reproduce qualitatively the salient features of Covid-19, as experienced in very recent years. Future research should be aimed at a quantitative comparison of the mathematical results with the medical data collected during the recent pandemic, in order to organize also them in a more systematic way. Indeed, available data are limited, incomplete, and often heterogeneous. Therefore, researchers, who aimed to carry out a detailed comparison between model predictions and a realistic epidemic scenario, used also optimization techniques and specific numerical methods to take into account the high degree of data uncertainty (Albi et al. 2022). All these issues that should be handled with particular care justify the qualitative epidemiological study reported in this paper, postponing an adequate quantitative analysis to future investigations.

Appendix: Preliminaries on Boltzmann Interaction Operators for Multi-species Systems

The classical kinetic theory for N interacting populations is based on a system of evolution equations for the distribution function of each constituent $f_i(t, \mathbf{x}, \mathbf{v})$, $i = 1, \ldots, N$, typically depending on time $t \in \mathbb{R}_+$, on space $\mathbf{x} \in \mathbb{R}^d$ (with $d = 1, 2, 3$), and on a kinetic variable $\mathbf{v} \in \Sigma$, specific of the considered frame. Just as an example, $\mathbf{v} \in \mathbb{R}^3$ denotes the molecular velocity in gas dynamics (Cercignani 1988), $v \in \mathbb{R}^+$ the individual wealth in kinetic models for a market economy (Cordier et al. 2005), $v \in [0, 1]$ the cellular activity in Ramos et al. (2019), and $v \in \mathbb{R}$ the individual viral load in the present paper.

In this Appendix, we consider a system of 4 populations that, besides all classical binary interactions (without transfers), can also give rise to the following (reversible) interaction with transfers:

$$1 + 2 \rightleftarrows 3 + 4, \tag{A.1}$$

where a pair of agents of populations (1, 2) moves to populations (3, 4), respectively, or vice versa.

In such multi-species frame, the space-homogeneous Boltzmann equation for the distribution f_i reads as

$$\frac{\partial f_i}{\partial t}(t, \mathbf{v}) = \sum_{j=1}^{4} Q^{ij} + \overline{Q}^i \qquad i = 1, \ldots, 4, \tag{A.2}$$

where Q^{ij} is the binary operator for interactions without transfers involving a pair of species (i, j), while $\overline{Q}^i$ is an interaction operator describing the effects on species i due to the transfers (A.1).

In general form, the operator Q^{ij} can be written as

$$Q^{ij} = \left\langle \int_{\Sigma} I_{ij}^{ij}(\mathbf{v}, \mathbf{w}, \eta) \left[f_i(\mathbf{v}') \, f_j(\mathbf{w}') - f_i(\mathbf{v}) \, f_j(\mathbf{w}) \right] d\mathbf{w} \right\rangle \tag{A.3}$$

where $(\mathbf{v}, \mathbf{w})$ are the pre-interaction kinetic variables of agents (i, j), and $(\mathbf{v}', \mathbf{w}')$ are the post-interaction kinetic variables. The function $I_{ij}^{ij}(\mathbf{v}, \mathbf{w}, \eta)$ in the kernel of the Boltzmann operator takes into account the probability that the considered interaction $(\mathbf{v}, \mathbf{w}) \to (\mathbf{v}', \mathbf{w}')$ occurs. The angular brackets denote the integration over all additional parameters η appearing in the interaction rule (namely in $\mathbf{v}', \mathbf{w}'$) or in the kernel I_{ij}^{ij}. For instance, in gas dynamics one has to integrate over the impact angles of the collision (typically, over the direction of the post-collision relative velocity) (Cercignani 1988; Giovangigli 1999), while in interactions involving human beings one has to integrate over proper random variables taking into account non-deterministic effects (Cordier et al. 2005; Pareschi and Toscani 2013).

Transfer operators $\overline{Q}^{i}$ may be cast in a similar form

$$\overline{Q}^{i} = \left\langle \int_{\Sigma} I_{ij}^{hk}(\mathbf{v}, \mathbf{w}, \eta) \left[f_h(\mathbf{v}') \, f_k(\mathbf{w}') - f_i(\mathbf{v}) \, f_j(\mathbf{w}) \right] \mathrm{d}\mathbf{w} \right\rangle \tag{A.4}$$

where, according to (A.1), the indices are such that

$$(i, j, h, k) \in \{(1, 2, 3, 4), (2, 1, 4, 3), (3, 4, 1, 2), (4, 3, 2, 1)\}.$$

The kernel I_{ij}^{hk} could involve also suitable Heaviside functions: In gas dynamics, they account for the fact that an endothermic reaction cannot occur if the kinetic energy of the ingoing molecules is not enough (Giovangigli 1999; Rossani and Spiga 1999), and in socio-economic problems they guarantee that post-interaction kinetic variables remain in the admissible domain (Cordier et al. 2005).

In the pertinent literature, different collision-like operators have been proposed. Specifically, for a single monatomic gas, one can prove the equivalence of the following formulations of the Boltzmann collision operator (Boffi et al. 1990).

(a) Kinetic formulation:

$$Q(f, f)(\mathbf{v}) = \int_{\mathbb{R}^3} \mathrm{d}\mathbf{w} \int_{\mathbb{S}^2} g \, I(g, \chi) \left[f(\mathbf{v}') f(\mathbf{w}') - f(\mathbf{v}) f(\mathbf{w}) \right] \mathrm{d}\hat{\Omega}'. \tag{A.5}$$

In the classical form, the Boltzmann collision term is a quadratic operator provided by the difference between a gain and a loss contribution (Cercignani 1988). In the gain term, distributions are depending on pre-collision velocities $\mathbf{v}', \mathbf{w}'$ corresponding to the post-collision ones $\mathbf{v}, \mathbf{w}$. The relative velocity of the interacting particles is denoted by $\mathbf{g} = \mathbf{v} - \mathbf{w} = g \, \hat{\Omega}$. The differential scattering cross section $I(g, \chi)$ depends both on the relative speed and on the deflection angle of the relative motion

$\chi = \arccos(\hat{\Omega} \cdot \hat{\Omega}')$; in addition, the explicit form of the cross section is determined by the intermolecular interaction potential of the considered gaseous medium. For instance, inverse-power intermolecular potentials $V(d) = d^{-p}$ (where d denotes the intermolecular distance and $p > 1$) give $I(g, \chi) = g^{-4/p}\tilde{I}(\chi)$, so that in the particular case $p = 4$ (Maxwell molecules) the collision kernel $g\, I(g, \chi)$ is independent of g. In case of elastic collisions, preserving momentum and kinetic energy, post-collision velocities are uniquely determined in terms of the pre-collision ones, once the direction of the post-collision relative velocity is given.

(b) Waldmann formulation:

$$Q(f, f)(\mathbf{v}) = \int_{\mathbb{R}^3}\int_{\mathbb{R}^3}\int_{\mathbb{R}^3} W(\mathbf{v}', \mathbf{w}'; \mathbf{v}, \mathbf{w})[f(\mathbf{v}')f(\mathbf{w}') - f(\mathbf{v})f(\mathbf{w})]\, \mathrm{d}\mathbf{w}\mathrm{d}\mathbf{v}'\mathrm{d}\mathbf{w}'. \tag{A.6}$$

In this probabilistic formulation, proposed in Waldmann (1958), the kernel $W(\mathbf{v}', \mathbf{w}'; \mathbf{v}, \mathbf{w})$ represents the microscopic probability distribution for the collision process $(\mathbf{v}, \mathbf{w}) \to (\mathbf{v}', \mathbf{w}')$. Notice that in (A.6) the integrals range over all possible values of the ingoing velocity of the partner molecule $\mathbf{w}$ and of the output velocity pair $\mathbf{v}'$, $\mathbf{w}'$.

(c) Scattering kernel formulation:

$$\begin{aligned} Q(f, f)(\mathbf{v}) = &\int_{\mathbb{R}^3}\int_{\mathbb{R}^3} \eta(\mathbf{v}', \mathbf{w}')\, A(\mathbf{v}', \mathbf{w}'; \mathbf{v})\, f(\mathbf{v}')f(\mathbf{w}')\, \mathrm{d}\mathbf{v}'\, \mathrm{d}\mathbf{w}' \\ &- f(\mathbf{v}) \int_{\mathbb{R}^3} \eta(\mathbf{v}, \mathbf{w})\, f(\mathbf{w})\, \mathrm{d}\mathbf{w} \end{aligned} \tag{A.7}$$

which is related to the Waldmann one by

$$\eta(\mathbf{v}, \mathbf{w}) =: \int_{\mathbb{R}^3}\int_{\mathbb{R}^3} W(\mathbf{v}', \mathbf{w}'; \mathbf{v}, \mathbf{w})\, \mathrm{d}\mathbf{v}'\, \mathrm{d}\mathbf{w}' \tag{A.8}$$

and

$$\eta(\mathbf{v}', \mathbf{w}')\, A(\mathbf{v}', \mathbf{w}'; \mathbf{v}) =: \int_{\mathbb{R}^3} W(\mathbf{v}', \mathbf{w}'; \mathbf{v}, \mathbf{w})\, \mathrm{d}\mathbf{w}. \tag{A.9}$$

It can be easily checked that the transition probability $A(\mathbf{v}', \mathbf{w}'; \mathbf{v})$ satisfies the properties

$$A(\mathbf{v}', \mathbf{w}'; \mathbf{v}) = A(\mathbf{w}', \mathbf{v}'; \mathbf{v}), \tag{A.10}$$

$$\int_{\mathbb{R}^3} A(\mathbf{v}', \mathbf{w}'; \mathbf{v})\, \mathrm{d}\mathbf{v} = 1. \tag{A.11}$$

Analogous formulations and equivalence results also hold for mixtures of different monatomic constituents (Spiga et al. 1985). The scattering kernel formalism remains valid also with stochastic collisions, occurring for instance in social or economic problems, as in simple market economies or in epidemic models. For stochastic interactions, in which $A(\mathbf{v}', \mathbf{w}'; \mathbf{v})$ satisfies only the relationships (A.10) and (A.11), with $\mathbf{v}', \mathbf{w}', \mathbf{v}$ independent variables, one cannot expect conservation of momentum and energy. In the literature of kinetic equations for socio-economic sciences, it is shown the equivalence between the collision-like Boltzmann equation and Markovian jump-processes, described by transition probabilities related to the Waldmann formulation of the Boltzmann equation (Loy and Tosin 2020).

Acknowledgements M.B. and S.L. are supported by GNFM of INdAM, Italy. Moreover, M.B. thanks the support by the University of Parma through the project *Collective and self-organized dynamics: kinetic and network approaches* (Bando di Ateneo 2022 per la ricerca - PNR - PNRR - NextGenerationEU), and by the Italian Ministry MUR through the projects *Integrated Mathematical Approaches to Socio-Epidemiological Dynamics* (PRIN 2020JLWP23) and *Mathematical Modelling for a Sustainable Circular Economy in Ecosystems* (PRIN 2022 PNRR P2022PSMT7, also funded by the European Union - NextGenerationEU).

Funding Open access funding provided by Politecnico di Milano within the CRUI-CARE Agreement.

Data availability The data that support the findings of this study are available from the corresponding author.

Declarations

Conflict of interest The authors declare that they have no conflict of interest.

References

Albi, G., Bertaglia, G., Boscheri, W., Dimarco, G., Pareschi, L., Toscani, G., Zanella, M.: Kinetic modelling of epidemic dynamics: Social contacts, control with uncertain data, and multiscale spatial dynamics. In: Bellomo, N., Chaplain, M. A. J. (eds.) Predicting Pandemics in a Globally Connected World, Vol. 1, pp. 43–108, Birkhäuser (2022)

Ball, P.: The physical modelling of society: a historical perspective. Phys. A **314**, 1–14 (2002)

Bellomo, N., Bingham, R., Chaplain, M.A., Dosi, G., Forni, G., Knopoff, D.A., Lowengrub, J., Twarock, R., Virgillito, M.E.: A multiscale model of virus pandemic: heterogeneous interactive entities in a globally connected world. Math. Mod. Methods Appl. Sci. **30**, 1591–1651 (2020)

Bernoulli, D.: Essai d'une nouvelle analyse de la mortalité causée par la petite vérole. Mém. Math. Phys. Acad. Roy. Sci., Paris, 1–45, In Histoire de l'Academie Royale des Sciences (1766)

Bertaglia, G., Pareschi, L.: Hyperbolic models for the spread of epidemics on networks: kinetic description and numerical methods. ESAIM: Math. Model. Num. Anal. **55**, 381–407 (2021)

Boffi, V.C., Protopopescu, V., Spiga, G.: On the equivalence between the probabilistic, kinetic, and scattering kernel formulations of the Boltzmann equation. Phys. A **164**, 400–410 (1990)
Boscheri, W., Dimarco, G., Pareschi, L.: Modeling and simulating the spatial spread of an epidemic through multiscale kinetic transport equations. Math. Models Methods Appl. Sci. **31**, 1059–1097 (2021)
Boyton, R.J., Altmann, D.M.: The immunology of asymptomatic SARS-CoV-2 infection: What are the key questions? Nat. Rev. Immunol. **21**, 762–768 (2021)
Buonomo, B., Giacobbe, A.: Oscillations in SIR behavioural epidemic models: the interplay between behaviour and overexposure to infection. Chaos, Solitons Fract. **174**, 113782 (2023)
Cercignani, C.: The Boltzmann Equation and Its Applications. Springer, New York (1988)
Cordier, S., Pareschi, L., Toscani, G.: On a kinetic model for a simple market economy. J. Stat. Phys. **120**, 253–277 (2005)
Degond, P., Pareschi, L., Russo, G. (Eds.): Modeling and Computational Methods for Kinetic Equations. Springer Science & Business Media (2004)
Delitala, M.: Generalized kinetic theory approach to modeling spread and evolution of epidemics. Math. Comput. Model. **39**, 1–12 (2004)
De Lillo, S., Delitala, M., Salvatori, M.C.: Modelling epidemics and virus mutations by methods of the mathematical kinetic theory for active particles. Math. Models Methods Appl. Sci. **19**, 1405–1425 (2009)
Della Marca, R., Loy, N., Tosin, A.: A SIR-like kinetic model tracking individuals' viral load. Netw. Heterog. Med. **17**, 467–494 (2022)
Della Marca, R., Loy, N., Tosin, A.: An SIR model with viral load-dependent transmission. J. Math. Biol. **86**, 61 (2023)
Dimarco, G., Pareschi, L., Toscani, G., Zanella, M.: Wealth distribution under the spread of infectious diseases. Phys. Rev. E **102**, 022303 (2020)
Dimarco, G., Perthame, B., Toscani, G., Zanella, M.: Kinetic models for epidemic dynamics with social heterogeneity. J. Math. Biol. **83**, 4 (2021)
Dimarco, G., Toscani, G.: Kinetic modeling of alcohol consumption. J. Stat. Phys. **177**, 1022–1042 (2019)
D'Onofrio, A., Manfredi, P.: Behavioral SIR models with incidence-based social-distancing. Chaos, Solitons Fract. **159**, 112072 (2022)
Fraia, M., Tosin, A.: The Boltzmann legacy revisited: kinetic models of social interactions. Mat. Cult. Soc. **5**, 93–109 (2021)
Giordano, G., Blanchini, F., Bruno, R., Colaneri, P., Di Filippo, A., Di Matteo, A., Colaneri, M.: Modelling the Covid-19 epidemic and implementation of population-wide interventions in Italy. Nat. Med. **26**, 855–860 (2020)
Giovangigli, V.: Multicomponent Flow Modeling. Series on Modeling and Simulation in Science, Engineering and Technology, Birkhäuser, Boston (1999)
Hethcote, H.W.: The mathematics of infectious diseases. SIAM Rew. **42**, 599–653 (2000)
Kermack, W.O., McKendrick, A.G.: Contributions to the mathematical theory of epidemics. Proc. R. Soc. London, Ser. A **115**, 700–721 (1927)
Kermack, W.O., McKendrick, A.G.: Contributions to the mathematical theory of epidemics. II-The problem of endemicity. Proc. R. Soc. London, Ser. A **138**, 55–83 (1932)
Kermack, W.O., McKendrick, A.G.: Contributions to the mathematical theory of epidemics. III.-Further studies of the problem of endemicity. Proc. R. Soc. Lond. Ser. A **141**, 94–122 (1933)
Kim, D., Quaini, A.: Coupling kinetic theory approaches for pedestrian dynamics and disease contagion in a confined environment. Math. Models Methods Appl. Sci. **30**, 1893–1915 (2020)
Lambert, J.H.: Die Tödlichkeit der Kinderblattern. Beyträge zum Gebrauche der Mathematik und deren Anwendung. Buchhandlung der Realschule, Vol. 3, Berlin, Germany (1772)
Loy, N., Tosin, A.: Markov jump processes and collision-like models in the kinetic description of multi-agent systems. Commun. Math. Sci. **18**, 1539–1568 (2020)
Pareschi, L., Toscani, G.: Interacting Multiagent Systems: Kinetic equations and Monte Carlo methods. Oxford University Press, Oxford (2013)
Patriarca, M., Chakraborti, A.: Kinetic exchange models: from molecular physics to social science. Amer. J. Phys. **81**, 618–623 (2013)
Ramos, M.P., Ribeiro, C., Soares, A.J.: A kinetic model of T cell autoreactivity in autoimmune diseases. J. Math. Biol. **79**, 2005–2031 (2019)
Ross, R.: The Prevention of Malaria. John Murray, London (1911)

Rossani, A., Spiga, G.: A note on the kinetic theory of chemically reacting gases. Phys. A **272**, 563–573 (1999)

Siettos, C.I., Russo, L.: Mathematical modeling of infectious disease dynamics. Virulence **4**, 295–306 (2013)

Spiga, G., Nonnenmacher, T., Boffi, V.C.: Moment equations for the diffusion of the particles of a mixture via the scattering kernel formulation of the nonlinear Boltzmann equation. Phys. A **131**, 431–448 (1985)

Stephenson, E., et al.: Single-cell multi-omics analysis of the immune response in Covid-19. Nat. Med. **27**, 904–916 (2021)

Toscani, G.: Statistical description of human addiction phenomena. In: Nota, A., Albi, G., Merino-Aceituno, S., Zanella, M. (eds.) Trails in Kinetic Theory: Foundational Aspects and Numerical Methods. Springer, Berlin (2020)

Waldmann, L.: Transporterscheinungen in gasen von mittlerem druck. In: Flügge, S. (ed.) Handbuch der Physik, vol. 12, pp. 295–514. Springer Verlag, Berlin (1958)

Wilmes, P., Zimmer, J., Schulz, J., Glod, F., Veiber, L., Mombaerts, L., Rodrigues, B., Aalto, A., Pastore, J., Snoeck, C.J., Ollert, M., Fagherazzi, G., Mossong, J., Goncalves, J., Skupin, A., Nehrbass, U.: SARS-CoV-2 transmission risk from asymptomatic carriers: Results from a mass screening programme in Luxembourg. Lancet Region. Health-Eur. **4**, 100056–9 (2021)

Zhang, S.X., Marioli, F.A., Gao, R., Wang, S.: A second wave? What do people mean by Covid waves? A working definition of epidemic waves. Risk Manag. Healthc. Polic. **14**, 3775–3782 (2021)

Zhang, X., Su, T., Jiang, D.: Dynamics of a stochastic SVEIR epidemic model incorporating general incidence rate and Ornstein–Uhlenbeck process. J. Nonlinear Sci. **33**, 76 (2023)

Zhang, X.-B., Zheng, L.: Complex dynamics of a stochastic SIR epidemic model with vertical transmission and varying total population size. J. Nonlinear Sci. **33**, 108 (2023)

Zhu, Q., Xu, Y., Wang, T., Xie, F.: Innate and adaptive immune response in SARS-CoV-2 infection-current perspectives. Front. Immunol. **13**, 1053437 (2022)